Organic nanoparticle tracking during pharmacokinetic studies

Samuel Bonnet, Rana Elfatairi, Florence Franconi, Emilie Roger, Samuel Legeay

Organic Nanoparticles Tracking During Pharmacokinetic Studies

Bonnet Samuel (1), Elfatairi Rana (2), Franconi Florence (1-2), Roger Emilie (2) & Legeay Samuel (2)*

Université d'Angers, PRISM, SFR ICAT, Plate-forme de recherche en imagerie et spectroscopie multi-modales, Angers F-49000, France

2 Université d'Angers, Inserm, CNRS, MINT, SFR ICAT, Angers F-49000, France
*Author for correspondence

Keywords: Organic nanoparticles; biodistribution; pharmacokinetics; integrity; quantitative methods; imaging methods; multimodal; FRET; in vivo; nanomedicine

Abstract

To understand how nanoparticles (NPs) interact with biological barriers and to ensure they maintain their integrity over time, it is crucial to study their *in vivo* pharmacokinetic (PK) profiles. Many methods of tracking have been used to describe *in vivo* fate of NPs and to evaluate their PKs and structural integrity. However, they do not deliver the same level of information and may cause misinterpretations. Here, we review and discuss the different methods for *in vivo* tracking of organic NPs. Among them, *Förster resonance energy transfer* (FRET) presents a great potential to track NPs integrity. However, FRET still needs validated methods to extract and quantify NPs in biological fluids and tissues.

Published in Nanomedicine

DOI 10.2217/nnm-2021-0155

1 - Introduction

Recently, nanoparticles (NPs) have gained great attention in the field of drug delivery due to their ability to deliver personalised and efficient treatments with fewer side effects. Personalised medicine depends on using *ex vivo* and *in vivo* data taken from both patient and from disease-specific characteristics. Using image-guided nanoparticles as drug delivery systems containing both drugs and the imaging agents within the same formulation allow to evaluate how well is the specific targeting to the pathologic sites. This allows to have a better patient response to nanoparticle-based interventions.[1] Moreover, NPs may cross many biological barriers, allow hydrophobic drugs delivery and site specific targeting.[2] Despite the presence of many publications on NPs advantages, only a small number of NPs-based therapeutics (called nanomedicine) is reaching the market, and accepted for clinical use. This could be explained by the complex behaviour of NPs and lack of information about their interaction with biological systems.[3–5] Indeed, encapsulated drugs in NPs have a distinct behaviour compared to conventional drugs. Thus, it is difficult to predict the NPs behaviours from loaded-drug PK studies.[2,6,7] Additionally, it is essential to perform PK studies for NPs to understand and predict their own fate and behaviour which can be directly correlated with their efficacy and side effects.[6,8] Among nanoparticles widely used in medicine, organic NPs is one of the most promising systems for drug delivery. Organic NPs include liposomes, polymeric micelles, polymeric or lipid-based nanoparticles (nanospheres and nanocapsules), and dendrimers (figure 1).[9]

Liposomes consist of an aqueous cavity surrounded by one or several phospholipid bilayer membranes. Due to their high versatility, they can encapsulate both hydrophilic and hydrophobic compounds.[13] Polymeric micelles (PMs) are formed from amphiphilic copolymers that self-assemble into a core-shell structure in aqueous environment and can encapsulate hydrophobic drugs.[14–16] Nanoparticles (including nanocapsules or nanospheres) are polymeric nanoparticles or lipids nanoparticles (lipid core present under solid matrix or liquid oily core surrounded by surfactant shell) and can encapsulate both hydrophilic or lipophilic drugs.[13,17] Dendrimers are hyperbranched polymeric macromolecules having a well-defined architecture of three main domains: *i)* an inner core, *ii)* branches that emerge from the core, *iii)* terminal functional groups.[18,19]

Currently, multiple methods have been used for NPs tracking in biological systems after *in vivo* administration. Some of them allow for the quantification of NPs using analytical methods after organs sampling but they often require animal sacrifice and make them not suitable for longitudinal follow-up. Other less invasive methods, using whole body imaging systems, allow for the localisation of NPs into organs during time, but they often suffer from uncertainties in the quantification of NPs. These uncertainties can be due to factors like a lack of spatial resolution and/or specificity, signal dependencies with the molecular environment of the probes and/or the experimental protocols settings, etc. In addition, encapsulation of the free drug in a nanoparticle enhances its pharmacological and pharmaceutical characteristics via prolongation of its circulation time, better targeting, enhancing its efficacy, prevention of drug resistance, lower immunogenicity and toxicity.[20,21] At the same time to deliver an effect, the drug should be released from the nanoparticle to the site of action. Thus, it is important to have detection methods enabling to distinguish the drug in both encapsulated and free state. Especially that most PK studies in the past 20 years have always been focused on the determination of the total drug concentration and not the nanoparticle

itself.[22] To sum up, each of these methods does not deliver the same level of information and may lead to misinterpretations of the NPs

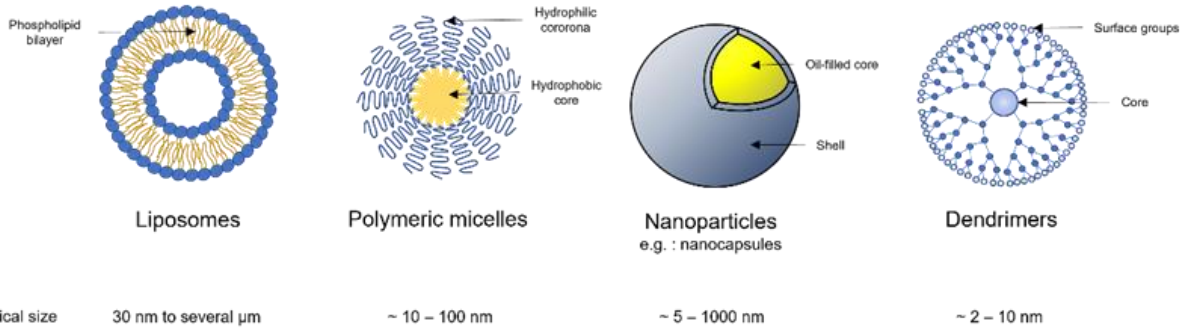

*figure 1. Organic nanoparticle*s

pharmacokinetic profiles. This review compares the different methods used for organic NPs tracking after *in vivo* administration and highlight their relevance to study NPs pharmacokinetics and structural integrity.

2 – Drug concentration measurements

Most of the time, a new nanoformulation is employed to improve the pharmacokinetic properties of a drug after its administration. The biodistribution of NPs encapsulating a therapeutic compound can be evaluated by measuring the drug concentration in tissues. This concentration can be quantified with analytical methods (photometric, fluorimetric or mass spectroscopy detection…), eventually coupled with separation method (chromatographic method). Such measurements are considered as indirect techniques as they only allow for the biodistribution of the loaded drugs to be tracked. Moreover, this process involves tissue sample being prepared for solubilisation and drug extraction.[23] Additionally, an internal standard of showing the same chromatographic and mass spectrometric behaviour as the analyte should be used. Internal standard will enhance the accuracy and precision of quantitation together with the robustness of the established analytical method.[24]

2.1 Sample preparation

Sample treatment is an important step for the analytical dosage of encapsulated drugs inside NPs after *in vivo* administration, to obtain purified sample.[24]

One method of purification is solid phase extraction (SPE) which consists of a particulate or monolithic sorbent made of an inert material (e.g. polypropylene) filled into a cartridge (short-length column) or packed in a thin disc. The plasma sample of interest passes through this column where either the free or the encapsulated drug is retained on the selected sorbent and then eluted.[25–27] After SPE treatment, samples are purified, with suitable analyte concentration and a low signal-to-noise (S/N) ratio between the screened plasma and the LLOQ (lower limit of quantification) samples.[24] For example, in order to optimise an amphotericin-B dosage after intravenous administration, Deshpande NM *et al.* added liposomal amphotericin B (L-AMP) and free amphotericin B to human plasma samples which were passed through HLB (hydrophilic lipophilic balance) cartridge. Free drug was retained, and the liposomal-amphotericin B was eluted. Then, eluted L-AMP was treated with chloroform, DMSO and acetonitrile and sonicated to break the liposomes and solubilise Amphotericin B. The amount of free AMP and encapsulated AMP into liposome was determined *via* liquid chromatography-mass spectrometry (LC-MS/MS).[27]

Another blood sample and tissue homogenates treatment method is protein precipitation (PP) technique. For example, addition of methanol to liposomal-encapsulated prednisolone phosphate lead to both complete liposome rupture and protein precipitation.[28] This PP is beneficial in preventing interferences caused by biological artefacts. However, improper noise level is often generated and the PP technique is at risk of drug degradation, meaning that a decrease in the percentage of recovery can be observed.[24,29]

The last method that was involved in blood sample and tissue homogenates pretreatment is liquid-liquid extraction (LLE) which is used to separate the drug from the biological matrix. This leads to the production of clean samples with comparatively lower noise levels.[24] For example, encapsulated doxorubicin (DOX) in oleyl hyaluronan (HA-C18:1) polymeric micelles was quantified in mouse plasma after LLE by a mixture of chloroform/methanol with a percentage of recovery between 91.3% and 107.7% and a precision between 1.5% and 6.5%.[30] In any case, after all methods of purification, the drug should be quantified with adapted analytical methods.

2.2 High performance liquid chromatography (HPLC) analysis

HPLC is an improved type of liquid chromatography beneficial in the separation of a complex mixture of molecules found in biological systems.[31] HPLC allows a higher proficient separation than conventional gravity-flow liquid chromatography due to the employment of small beads in the stationary phase fulfilling fine and uniform packing. In addition, high pressure to push the mobile phase or the solvent through the stationary phase is applied realising better resolution and faster separation.[32,33]

To quantify drugs, HPLC can be coupled with different types of detectors (UV, fluorescence, Photo Diode Array (PDA), mass spectrometer…). Absorbance detectors (UV, visible, PDA) report the optical characteristics of the drug after chromatographic separation by measuring the reduction or the reflection of the beam of light from the sample surface. Using Beer–Lambert Law, encapsulated drug concentration can be calculated after measuring the absorbance at a specific wavelength.[31,32] For example, bifendate (DDB) detection and accurate quantitation of DDB liposomal formulations in biological fluids were achieved using HPLC method coupled with a UV detector, resulting in a limit of quantitation (LOQ) of 20 ng/ml.[34] As another example, quercetin and piperine in dual-drug loaded nanostructured lipid carriers (NLCs) were detected and quantified using HPLC with a PDA detector. LOD was found to be 0.66 µg/mL and 0.33 µg/mL while the LOQ was 2.0 µg/mL and 1.0 µg/mL for quercetin and piperine respectively. These values were sufficient for accurate and precise determination of encapsulated quercetin and piperine pharmacokinetics profile.[35]

Fluorometric detectors are another type of detector that shows high sensitivity and specificity for fluorescent molecules. Thanks to their limits of detection able to reach the picomolar range, they are helpful in trace analysis although they have a smaller linear range.[33] For example, Cyanine-5 radiolabeled PAMAM Dendrimers (D-Cy5) were administered intravenously to neonatal rabbits to study their biodistribution *in vivo*. Major organs extract, blood and urine were analysed after 24h using HPLC coupled to a fluorescence detector. This method showed high levels of sensitivity with a low limit of detection (100 ng per gram of tissue).[36]

Mass spectrometry (MS) is a high-performance analytical method that employs generated mass-to-charge ratio (m/z) of ions for the identification and quantification of drugs.[33,37,38] Interestingly, MS can be used when other detection techniques as UV detection or fluorescence cannot be used due to absence of light-absorbing groups or fluorescent groups in the targeted molecule and LC-MS/MS is more specific and sensitive than

UV- or fluorescent detection.[34,39] Thus, coupling of LC with an MS is taken into consideration to obtain a full scan analysis by the mass determination.[31,38] For example, LC-MS was utilised to accurately quantify liposomal encapsulated prednisolone concentration in murine whole blood and liver. The limits of quantification were 99 nmol/L in blood and 0,53 nmol/g of liver for prednisolone. [29]

It is important to note that an internal standard can be used to provide a more accurate drug measurement. The internal standard consists of adding a known amount of a known drug (called internal standard) to each sample, including calibrators. Instead of basing the calibration on the absolute response of the analyte, the calibration including the internal standard uses the ratio of response between the analyte and the internal standard. An internal standard will benefit the method when there are multiple sample preparation steps, which is often the case with NPs dosage. However, the internal standard should be added as early in the process as possible and an optimisation of the method should be done to ensure the absence of interactions between the internal standard and the sample containing NPs.[40]

Each of these papers show that HPLC can have a good potential for indirect *in vivo* quantification of NPs, especially during PK studies. However, because analytical methods only quantify the drug, the pharmacokinetic profile which is described only corresponds to the encapsulated drug properties and does not reflect the pharmacokinetics of the NPs themselves. These widely used methods can evidence the effect of the nanoformulation of a drug on the pharmacokinetics of this drug but those results cannot be extrapolated to the pharmacokinetics of NPs. In addition, the sample preparation step absolutely requires a separation between the encapsulated drug and the free drug.

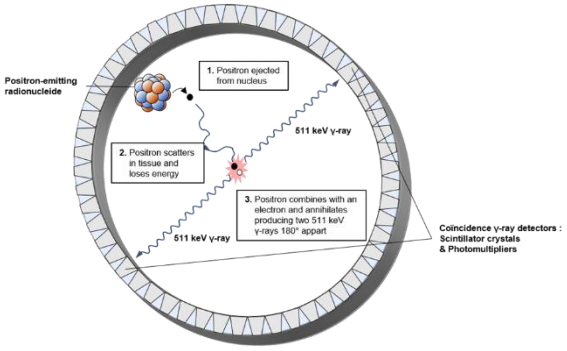

Figure 2 : Physics underlying PET (from 42)

3 - Nuclear Imaging

Nuclear imaging involves the application of radioactive substances. Positron emission tomography (PET) and single-photon emission computed tomography (SPECT) scans are the two most common imaging modalities in nuclear medicine. Despite some limitations like a moderate spatial resolution, a relatively high cost, or the exposure to ionising radiation, these techniques are often used in nanomedicine studies.[41]

3.1 Positron Emission Tomography (PET)

3.1.1 Basic principle of PET

Positron emission tomography (PET) is a non-invasive quantitative nuclear imaging technique able to generate three-dimensional images of living subjects using a positron-labelled tracer and a PET camera. The tracer is given to the subject, where positron emission leads to radionuclide decay in the body. Then, the collision that occurs between the produced positron and the nearby electron, leads to the formation of two 511 keV γ-rays split by 180 degrees (figure 2).

Scintillation detectors convert the coincidence high-energy photons into visible light recognised by photomultiplier tubes. These events are built into 3D image expressing the

spatial distribution of the tracer and revealing its concentration in the subject using mathematical reconstruction techniques and correction factors.[43,44] Several regions of interest (ROIs) are drawn on PET images and the regional concentration of the tracer is measured accurately at a picomolar level. Dynamic scan or a sequence of static scans can be used to measure the changes in the radionuclide concentration. Moreover, parameters such as time-activity curve (TAC) and the standardised uptake value (SUV) are used to quantify the radionuclide exposure and uptake.[43,45,46]

3.1.2 Radiolabeling of nanoparticles in PET

Generally, PET imaging needs a positron-emitting radionuclide within the NP, which is usually generated by an accelerator. Some elements as oxygen, nitrogen, and carbon have positron-emitting isotopes, which is beneficial to conserve biochemical characteristics of the native compound after labelling by direct substitution. However, these radionuclides have very short half-lives ($T_{1/2}$ ^{15}O : 122 sec ; $T_{1/2}$ $^{13\,N}$: 9.97 min ; $T_{1/2}$ $^{11\,C}$: 20.3 min) and require on-site generation *via* biomedical cyclotron. On the other hand, metal radionuclides such as $^{68\,Ga}$ and $^{62\,Cu}$ can be produced in a generator without the need of a cyclotron. Moreover, $^{68\,Ga}$ radionuclides have a longer half-life ($T_{1/2}$ $^{68\,Ga}$: 68.1 min ; $T_{1/2}$ $^{64\,Cu}$: 12.7 h).[44] Radiolabeling is achieved by radionuclide incorporation into the NP through a chemical reaction. Using $^{11\,C}$, $^{18\,F}$, and ^{124}I for radiolabeling is usually performed *via* organic chemistry reactions. While, labelling with metallic radioisotope as $^{64\,Cu}$, $^{68\,Ga}$ and $^{89\,Zr}$ is often done through chelation to the surface or the core of the NP.[43,47,48] Since NPs are meant to circulate for prolonged periods, chelation-based approaches are more reliable to convey radionuclides having longer half-lives that may preserve radioactivity for several days.[49] As a result, non-metallic radioisotopes having short half-life is less suitable for usage with NPs as it prevents multiple days biological processes to be followed.[45,46,50] Most of the time the chelation stability is tested by incubation in fetal bovine serum and physiological buffered solution (PBS). The fetal bovine serum simulates the proteinaceous environment in the circulation while PBS tests the chelator stability to retain the radionuclide.[49,51,52]

3.1.3 *In vivo* application of PET

Jai Woong Seo *et al.* chelated ^{64}Cu to the surface of PEGylated liposomes *via* ^{64}Cu-specific chelator called 6-[p – (bromoacetamido)benzyl]-1,4,8,11-tetraazacyclotetradecane-N,N′,N′′,N′′′-tetraacetic acid (BAT). BAT was first attached to an artificial lipid to form a BAT-Polyethylene glycol (PEG)-lipid at low temperature and mild operating settings. The resulting liposome was then incubated with $^{64}CuCl_2$ and $^{64\,Cu}$ labelled liposome was obtained. The incorporation yield was about 95% and the radiolabeling stability after 48h incubation in serum/PBS solution showed that more than 88% of the $^{64\text{-}Cu}$ label was still attached.[48]

On the other hand, a lipid-PEG-BAT chelator was incorporated into solid lipid nanoparticles (SLNs). After incubation with $^{64}CuCl_2$, SLN was successfully radiolabeled with 66.5% radiolabeling yield of $^{64\,Cu}$. After intravenous administration to mice, PET imaging was performed to quantitatively assess SLNs biodistribution. About 1.4h ^{64}Cu-SLNs half-life in the blood was obtained and almost 5-7% of injected dose per gram (ID/g) ^{64}Cu-SLNs remained in the liver 48 h post injection.[45]

In another study, Jan Marik *et al.* sequestered radiolabeled diglyceride, 3 – [18 F] fluoro-1, 2-dipalmitoylglycerol [[^{18}F]fluorodipalmitin ([^{18}F] FDP)] in the liposomal phospholipid layer. The formulation has been administered to Male Fischer rats *via* tail vein injection and PET scans have been used to reveal their biodistribution. Results showed that liposomal [$^{18\,F}$] FDP had a nearly constant blood level for around 90 minutes, with a peak concentration of 2.5 %ID/cc (percentage of injected dose per cubic centimetre). [53]

These studies show that PET imaging modality can be used for the quantification and the

biodistribution studies of NPs. Its picomolar sensitivity level makes this technique very interesting for a precise detection of radiolabeled organic nanoparticles in the whole body. However, because PET imaging requires radiolabeled NPs with an isotope, it is not well defined if the detection of the signal is due to the entire NPs or if the NPs are broken and only labelled part of NPs are detected. In addition, this technique suffers from a lack of resolution and often needs to be combined with other imaging modalities using X-rays (CT-imaging) or Nuclear Magnetic Resonance (MRI) to evaluate more precisely the biodistribution of NPs. Moreover, the main part of the production of PET radionuclides is dependent of an onsite cyclotron but such equipment remains not easily accessible today. Although there are some radionuclides which can be produced with a generator, their relative short half-lives make PET imaging a modality which is not completely suitable for longitudinal PK studies over the days.

3.2 Single photon emission computed tomography (SPECT)

3.2.1 Basic principle of SPECT

SPECT is a nuclear imaging method that employs gamma rays to examine biochemical changes, numbers of molecules within living subjects and their biodistribution *via* three-dimensional tracing of gamma emitters as Indium-111 (^{111}In), Iodine-123 (^{123}I), Galium-67 (^{67}Ga) or Technetium-99m (^{99m}Tc). SPECT has been one of the primary imaging techniques owing to the usage of ^{99m}Tc which can be easily achieved from ^{99}Mo/^{99m}Tc generators with a great radioactive decay and a relative low cost.[54,55] In SPECT, imaging of radioisotopes is performed *via* a gamma camera composed of a scintillation detector consisting of a collimator, a sodium iodide crystal and a set of multiplier tubes. Gamma rays of specific energies are produced upon radionuclide decay. Only gamma rays parallel to the collimator will be detected. Then, the crystal will stop these rays which they will be converted into photons. Afterwards, the photomultiplier tubes will turn these photons into an electrical signal proportional to the gamma ray, which finally reaches the detector. Gamma cameras get data in a single plane and the obtained images are usually two-dimensional representation of three-dimensional radioactivity biodistribution. Thus, the camera rotates around the subject obtaining different views to provide an approximation of the three-dimensional radioactivity using image reconstruction (figure S1).[54,56,57]

Unlike PET, SPECT can image various radionuclides within the same object. This is attributed to the distinctive energy emissions of SPECT radionuclides that can be determined simultaneously and independently. While, in PET all emitted photons throughout positron annihilation have the same 511 keV energy. This makes the detection of multiple radionuclides unlikely with standard PET scanners.[56] Since PET cameras depend on coincidence detection and do not necessitate collimators, SPECT shows lower sensitivity than PET. Nevertheless, both of them show similar resolution in preclinical implementations.[56]

3.2.2 Radiolabelling of nanoparticles in SPECT

Radiolabeling of NPs for SPECT imaging can be achieved by labelling them with radionuclides. SPECT allows non-invasive detection of NPs inside the living subject and real time biological processes follow-up. There are certain factors to take into consideration during radionuclide selection: to prevent any misinterpretation during the following up of NPs, radioisotope half-life should not be higher than the nanoparticle half-life itself. In this case, using ^{99m}Tc ($t_{1/2}$ = 6h) could be considered as a good choice. On the other hand, the radioisotope half-life should not be too short because it would become a limit factor to track long circulating NPs. In this case ^{111}In ($t_{1/2}$ = 2.8 days) would be a better option. Another factor is obtaining a stable radiolabelled complex with a similar activity to the initial NP by choosing a

suitable labelling method. Therefore, the incorporation of the radionuclide should be performed with the slightest changes to the parent compound structure. The stability of radionuclides requiring chelators to obtain stable radiolabeled conjugates should always be examined. Another critical factor, which is often neglected, is the possibility of radionuclide release from nanoparticles due to metabolic reactions as enzymatic dehalogenation, macrophage degradation and competition with endogenous metals. These reactions can lead to uptake of the "free" or "unchelated" radionuclides by different tissues and organs, which may lead to false data collection and misinterpretations of the images. [56]

3.2.3 *In vivo* application of SPECT

PEGylated dendrimer poly(amidoamine (PAMAM)-folic acid conjugate was radiolabeled with ^{99m}Tc. Acetylated dendrimer first reacted with diethylenetriamine pentaacetic acid (DTPA) bifunctional chelator to form a conjugate which is then labelled with ^{99m}Tc and ^{99m}Tc labelled PEGylated dendrimer PAMAM folic acid conjugate (^{99m}Tc-G5-Ac-pegFA-DTPA) was formed.[58] Micro-SPECT images after *i.v.* injection of ^{99m}Tc-dendrimers to KB-bearing *nude* mice showed γ radiation mainly located in kidneys, liver, and the tumour mass. Author attributed these results to the presence of folate receptors in these areas.[58]
In another study, Adrianus C. Laan *et al.* entrapped $^{111\ In}$ radiolabel in the core of polystyrene-*b*-poly (ethylene oxide) (PS-PEO) diblock copolymer micelles during micellar formation. This was achieved by using tropolone as lipophilic ligand. After injecting radiolabeled polymeric micelles to Balb/c-nu mice, SPECT biodistribution analysis was performed over 24h. Above 20% Injected dose/g was measured in the blood at 24h indicating the persistence of a large percentage of the micelles in the circulation. However, a lower level in most organs (heart, lungs, kidneys, stomach, duodenum and colon) was obtained compared to the level obtained in the liver and the spleen.[59]

These studies show that SPECT imaging is an interesting modality which allows the user to follow NPs in a whole body after injection. This technique can take its value over PET thanks to a wider range of clinically tested tracers which can be used for long-tracking pharmacokinetics studies. However, like PET imaging, SPECT suffers from a low image resolution, and it could be difficult to precisely locate the signal if it is not combined with a CT scan. Additionally, this technique does not allow to differentiate the tracking of full integrity NPs from broken NPs.

3.3 *Ex vivo* quantification of radiolabeled-NPs

Another way to quantify NP biodistribution is to harvest organs after administration of labelled NP, animal sacrifice and *ex vivo* locate or quantify labels concentration. This can be performed using radiolabeling in order to measure the activity in each organ using gamma counter.
For example, gamma counting was utilised post imaging to confirm organ distributions of solid lipid nanoparticles loaded with $^{64\ Cu}$ (^{64}Cu-SLNs) 48h after injection.[45] PET and gamma counting demonstrated that approximately 5−7% ID/g ^{64}Cu-SLNs remained in the liver at 48 h post injection. These results indicated that the biodistribution of ^{64}Cu-SLNs can be quantitatively evaluated by *in vivo* PET imaging and *ex vivo* gamma counting. Another study assessed the biodistribution of ex vivo radiolabeled-micelles. [59] The authors founded significant blood circulation up to at least 24 h post injection, with low accumulation in most organs except for the liver and spleen.
These studies show that *ex vivo* characterisation of biological fluid or tissue sampled after *in vivo* radiolabeled-NP administration can be informative about their *in-vivo* pharmacokinetic biodistribution. An *in-vivo* observation combined with an *ex vivo* quantification of radiolabeled-NP gives a relatively good snapshot of the PK at the sampling time thanks to the excellent sensitivity of nuclear imaging techniques. However, if blood sampling can be

reiterated, organs sampling (brain, heart, liver, spleen…) require animal sacrifice and therefore do not allow longitudinal follow-up. Moreover, these nuclear imaging techniques do not allow to differentiate the tracking of full integrity NPs from broken NPs.

4 – Computed Tomography

4.1 Basic principle of CT

Computed tomography (CT) is a radiological technique that employs X-rays (ionising radiation with a wavelength of ~0.01–10 nm) to generate a three-dimensional, cross-sectional tissue image.[60] CT scanners are composed of an X-ray tube, a unit for detection, image reconstruction system, collimators and filters. To generate X-rays, a high voltage is applied within the X-ray tube allowing the acceleration of electrons from heated cathode towards the anode. Then, X-rays cross through the object where they get attenuated (absorbed and scattered) which leads to loss of the X-ray intensity.[60–62] Changes in the radiation intensities arising from different attenuation of X-rays across tissues provide information about the tissue density and its structure.[62,63]

4.2 Labelling of nanoparticles for CT

Although different tissue types have different contrasts, getting a high-quality image and identifying the interface between adjacent tissues remains a challenge. [61,63] To solve this problem, contrast agents are used to improve the CT sensitivity and provide better differentiation between tissues. These contrast agents are elements that show high atomic numbers, and consequently a high electron number that allows a more effective X-ray attenuation. The usually used contrast agents include iodine or barium-based agents.[61] Recently, CT has been used to follow the biodistribution of NPs *in vivo* for which electron-dense elements are contained into NPs allowing their visualisation and differentiation in the tissues. The commonly used contrast agents incorporated into NPs are iodine [64–66], gold [23,67,68], and bismuth [69]. Additionally, other elements including gadolinium [70], platinum [71], and tantalum [72] can also be used. To incorporate these contrast agents in NPs, they can be either loaded in the core of NPs, grafted *via* a chemical bond to the NP surface or inserted onto the NP membrane.[73,74] Furthermore, CT can be combined with either PET or SPECT to benefit from the functional information provided by PET or SPECT together with the high spatial resolution and anatomic information from CT.[75]

4.2 *In vivo* application of CT

CT has been used to study the biodistribution of various NPs *in vivo* such as nanoemulsions [76], liposomes [77], micelles [78], dendrimers [68] and nanocapsules [66]. For example, in a study performed by Hallouard *et al.*, iodinated nanoemulsions were formulated and coated with PEG to provide a stealth effect. Then, this formulation was intravenously injected in *nude* mice and *in vivo* assay was performed using CT imaging. Results showed a high contrast effect indicating high residence time of the nanoemulsion in the blood pool.[76] Varga *et al.* combined CT with SPECT (SPECT/CT) to study the biodistribution of liposomes *in vivo*. The liposomal surface was firstly labelled by adding thiol group which was then employed to bind with Tc-tricarbonyl complex. Labelling efficiency was examined using size exclusion chromatography and was found to be 95%. Also, the stability of labelled liposomes was tested in bovine serum albumin and was found to be 94% over 2 hours. $^{99\,m}$Tc-labelled liposomes were then injected in the tail vein of BALB/c mice and 99mTc-tricarbonyl complex only was also injected as a control. SPECT/CT was then employed to study the biodistribution profile of the organs and the blood at different time points. It was found that $^{99\,m}$Tc-labelled liposomes had a fast clearance from the blood and high uptake in the liver and spleen.[79] These studies show how CT scan can be used for organic NPs tracking. This whole-body

imaging technique is informative thanks to its good spatial resolution in comparison with PET or SPECT and is well suited for imaging bones and tumours. However, methods using CT have a low sensitivity and are not suited for soft tissues imaging or longitudinal studies as it needs the use of ionising rays. Moreover, CT scan does not allow to differentiate the tracking of full integrity NPs to broken NPs.

5 - Magnetic Resonance Imaging (MRI)

5.1 Basic principle of MRI

Magnetic resonance Imaging (MRI) is a noninvasive and non-ionising imaging technique based on nuclear magnetic resonance principles which enables deep tissue exploration and high spatial resolution. MR images are built from signal originating from hydrogen nuclei present in hydrogen-rich compounds in the body: water and lipids. A strong external magnetic field is applied to polarise the sample. Then, a radiofrequency pulse is applied leading to the nuclei excitation. When the radiofrequency pulse is stopped, the hydrogen nuclei transit from excited to ground state, known as relaxation phenomena.[80] There are two main relaxation processes: longitudinal relaxation characterised by T_1 (longitudinal relaxation time constant) and transverse relaxation characterised by T_2 (transverse relaxation time constant).[81] MRI contrast images result from intrinsic tissue difference in water hydrogen nuclei T_1 and T_2 relaxation times.

5.2 Labelling of nanoparticles for MRI

To improve MRI sensitivity and specificity, contrast agent (CA) should be used to enhance image contrast and thus to label NPs. The MRI contrast agents mainly act by altering T_1 and T_2 relaxation times of water molecules in close proximity to the contrast agent.[82] Their effect is indirect as the signal is still originating from the water hydrogen nuclei. The most commonly used contrast agents are paramagnetic chelates of the gadolinium ion (Gd^{3+}) and superparamagnetic iron oxide particles (SPIO) as shown in figure 3. In case of gadolinium paramagnetic agents, shortening of longitudinal T_1 relaxation time is predominantly achieved and a "bright" or positive contrast is produced in T_1-weighted images. As its relaxation mechanism is mainly based on the coordination of water molecules to the Gd ion, regularly exchanged with other surrounding water molecules (inner sphere effect), Gd ion access to water molecules must be preserved even when carried by the NP to induce image contrast. In case when SPIOs are used, shortening of transverse T_2 relation time is obtained and a "dark" or negative contrast is formed.[80] The long-distance effect of SPIO,

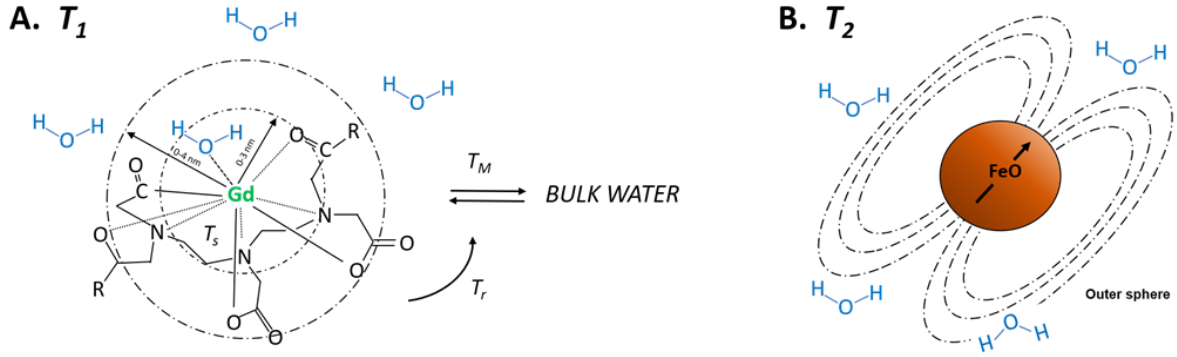

Figure 3 (A) Gadolinium complex interaction with water leading to shortening T_1 relaxation. (B) Superparamagnetic iron oxide interaction with water leading to shortening T2 relaxation. Adapted from [83,84]

that locally alters the magnetic field through which water molecules diffuse (outer sphere effect), does not require such close interaction with water molecules compared to Gd based contrast agent (GdCA). Incorporation inside the NP is therefore possible without contrast losses. It should be noted that the precise quantification of GdCA or SPIO with MRI is tricky since the MR contrast strongly depends on either their concentration or on the parameters of the MR sequence. Depending on its concentration, CA effect can appear as an hypersignal or an hyposignal. For example, the same GdCA could appear white (hypersignal) or dark (hyposignal) depending on its concentration and on the MR sequence and parameters used.

Another type of MRI contrast agent is based on the chemical exchange saturation transfer (CEST) effect.
These contrast agents have to possess exchangeable hydrogen nuclei (endogenous compounds with amide or hydroxyl or exogenous paramagnetic agent…) that resonates at a specific frequency. By applying radiofrequency at this resonance frequency, a saturation is achieved. Then, this saturated nuclei can be transferred from the contrast agent to bulk water leading to a local water signal reduction appearing as hyposignal on images.[81,85,86] CEST agents offer many advantages as they allow the detection of several agents simultaneously by applying different absorption frequencies.[81] Moreover, non-metallic safe agents can be used as a probe by increasing exchangeable protons local concentration.[86,87] Once injected *in vivo*, contrary to Gd or SPIO, they are only visible when dedicated CEST acquisition sequence are applied.
Lastly, fluorine 19 contrast agents can be used to label NP because they offer a specific MR signature.[88] The signal is directly proportional to the concentration of nuclei but with a lower sensitivity than for hydrogen imaging.

5.3 *In vivo* application of MRI

Long circulating liposomes have been loaded with amphiphilic paramagnetic contrast agent Gd-DOTAMA together with the glucocorticoid prednisolone phosphate. DOTAMA is a DOTA-type chelating agents (DOTA = 1,4,7,10-tetraazacyclododecane-1,4,7,10-tetraacetic acid) which is used to decrease gadolinium toxicity.[83] This liposomal formulation has been administered intravenously to melanoma B16 bearing mice. MRI images were obtained at day 0 (at 2 and 6 h after injection) and then at day 1, 2, and 3. MRI allowed non-invasive visualisation of liposome biodistribution and monitoring of their anti-tumour activity *in vivo*. It was found that clearance organs, like the spleen and the liver, collect the liposomes rapidly during the first day after injection. This accumulation was indicated by long-term residual T_1 contrast observed even after 1 week. However, this high uptake by the spleen and the liver led to a reduction in the liposomal amount in the blood and consequently less tumour accumulation. This was evidenced by the marked decrease in the percentage of T_1 contrast measured in the tumour *versus* the two other organs.[89]

In another study, superparamagnetic iron oxide particles (SPIO) were enclosed in three different liposomal formulations; SUV (Small Unilamellar Vesicles), SUV-PEG (Small Unilamellar Vesicles sterically stabilised with Polyethylene Glycol) and REV (Reverse Phase Evaporation Vesicles) and administered to CC531 adenocarcinoma–bearing rats *via* tail vein injection. MRI images showed a strong decrease in the tumour signal intensity up to 48h in case of SUV-PEG liposomes compared to other liposomes. This signal reduction in T_2-weighted images implies SUV-PEG enrichment in the tumour, higher than for the other formulations. This might be explained by its protection from opsonisation (due to the presence of PEG) and its small size that help it leaving the blood capillaries. [90]
To illustrate the potential of CEST contrast agent for NP tracking, liposomes have been loaded with barbituric acid (BA). BA is

characterised by exchangeable protons resonating at 5 ppm frequency. BA loaded liposomes were administered to CT26 cells tumour bearing mice *via i.v.* tail to monitor their tumour uptake in the presence and absence of tumour necrosis factor-alpha (TNF-α). The results showed CEST contrast of 0.4% at 5 ppm BA frequency. While upon TNF-α co-administration, the contrast increased to 1.5% with better uniform intratumoral dissemination. CEST images allowed semi-quantitative analysis and tumour targeting evaluation of liposomes in the tumour.[87]

In addition, Fluorine-19 (^{19}F) MRI tracking of drug loaded liposomes has been performed *in vivo* in mice.[91] Fluorinated amphiphile dendrimers were incorporated into liposomes as well as doxorubicin to make them ^{19}F MRI-traceable at drug therapeutic concentration. *In vivo* biodistribution was monitored by ^{19}F MRI after intravenous injection in mice. This study showed that fluorinated amphiphile-based liposomes could be employed as a general platform for *in vivo* NPs tracking with ^{19}F MRI.

Responsive contrast agents, often called as smart, have also been designed to report on various biomarkers.[92] Their impact on the image is then modulated (relaxivities, water access…). These smart contrast agents can be used for *in vivo* drug release tracking. For example, paramagnetic contrast agent and drug can be co-loaded in a photothermal NP for hyperthermia chemotherapy of tumours monitoring.[92] The release of paramagnetic ions, concomitant to the drug's, can be visualised on the image by T_1 contrast modification due to the modification of water accessibility to the paramagnetic core.

All these studies show that MRI is a technique which can be used for *in vivo* tracking of NPs. MRI takes advantage from its excellent spatial resolution and multi-contrast abilities compared to nuclear imaging techniques. It allows for a precise localisation of the NPs into the organs of whole body. However, MRI is also known for its lack of sensitivity and it is often tricky to precisely quantify the amount of contrast agent accumulated into an organ, depending on the magnetic properties of the CA (relaxivity) and on the MR parameters of the imaging sequence (image weighting).

6 - Fluorescence imaging

6.1 Basic principle of fluorescence

Fluorescence depends on photon absorption, which relocates electrons from the ground state to the excited state and when the electron returns back to ground state it sends out photons known as fluorescence emission. This concept is employed in different techniques as optical fluorescence imaging and fluorescence microscopy. For these techniques, a fluorescent molecule having a specific excitation and emission wavelength absorbs a light energy (photon) and emits part of this light, which has a lower energy and longer wavelength known as stokes shift explained by Jablonski energy diagrams (figure 4).[93,94]

6.2 Incorporation of Fluorescent dyes in Nanoparticles

NPs require labelling with a fluorescent molecule to be tracked using fluorescence imaging techniques. Some drugs such as doxorubicin.[96], epirubicin.[97], ellipticine, or proteins are inherently fluorescent and can be directly followed. However, most NPs are labelled with a fluorescent molecule, and some examples of fluorescent molecule used for liposome, dendrimers or nanoparticles/nanocapsules are presented in table 1. Near-infrared dyes (i.e. IRDye®800 CW, XenoLight CF 750, and 1,1'-Dioctadecyl-3,3,3',3'-Tetramethylindotricarbocyanine Iodide (DiR) or

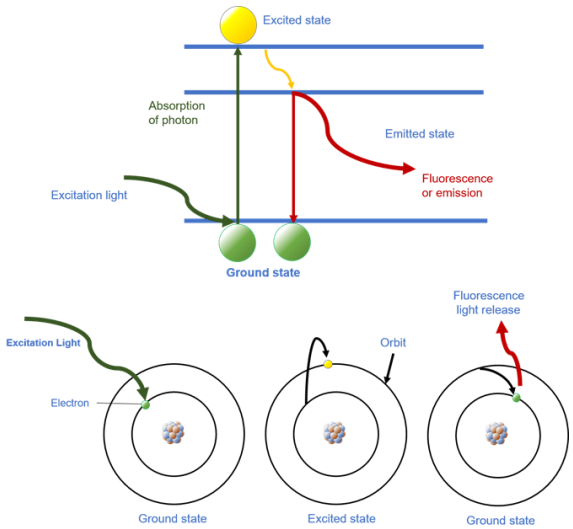

Alexa Fluor® 680 and 750 [98,99]) are the preferred fluorescent molecules to be used with fluorescence imaging for *in vivo* studies. Indeed, they encompass a suitable wavelength (650 to 900 nm) in which tissue absorption and auto fluorescence of collagen, elastin, and tryptophan are suppressed.

Figure 4 Schematic diagram showing the principle of fluorescence via Jablonski energy diagrams (above part). Adapted from [95]

Liposomes	Dendrimers	Nanoparticles
• Lipophilic carbocyanine tracer (i.e. 1,1'-dioctadecyl-3,3,3'3'-tetramethylindocarbocyanine perchlorate (DiD)). [100] • Carboxy-fluorescein.[101] • 1,2-distearoyl-sn-glycero-3 phosphoethanolamine (DSPE-ir623).[102]	• 1,1'-dioctadecyl-3,3,3'3'-tetramethylindocarbocyanine perchlorate (DiD).[103] • BODIPYfluorophore (4,4-difluoro-5,7-dimethyl-4-bora-3a, 4a-diaza-s-indacene-3-propionic acid).[104] • FITC (fluorescein isothiocyanate).[105]	• Itrybe.[106] • Texas-red-labelled insulin.[107] • Lipophilic carbocyanine tracer (DiD, DiI, DiO).[108] •Nile red derivative.[109]

Table 1: Examples of fluorescent molecules used to label liposomes, dendrimers and nanoparticles.

6.3 Whole body imaging

6.3.1 Fluorescence reflectance imaging (FRI)

FRI is a planar epi-illumination method, in which a light source and a detection device are located on the same side of the subject of interest. Accordingly, FRI system uses a single illumination design to obtain the subject image from a single view (figure S2).[110] The light source illuminates the subject by exciting the targeted fluorescent molecule with a specific wavelength after tissue penetration. Then, fluorescent molecule produces emission photons, which go back to the subject surface. A charge-coupled device (CCD) camera having a lens focused on the subject surface measures the emitted photons. This camera uses a spectral filter to detect the emission wavelength and reject other non-specific signals. Depending on which fluorescent molecule is used, FRI setups and CCD detection systems allow long-term detection (up to several months) and can monitor two or more fluorescent molecules at the same time.[98] In FRI, fluorescence signal is linearly correlated with fluorescent molecule concentration. However, nonlinear dependence generated from tissues affect FRI depth resolution, which makes quantitative analysis of fluorescent intensities difficult and only allows a semi-quantitative analysis.[94,98,110–112]

For example, inhaled polystyrene nanoparticles were fluorescently labelled with near infrared (NIR) fluorescence dye Itrybe. This hydrophobic asymmetric cyanine dye has a broad absorption (450 to 750 nm) and emission (650 to 900 nm) in the NIR region making it especially favourable for *in vivo* imaging. These NPs were intranasally administered to an ovalbumin-based allergic airway inflammation (AAI) model in SKH-1 mice. Fluorescence reflectance imaging (FRI) was employed 1 h, 5 h and 24 h after NP application. It was found that AAI lungs show considerably higher fluorescence intensities than lungs of control mice for at least 24 h due to an increased uptake of those NPs by macrophages. This study allowed semi-quantitative determination of the fluorescence intensity in AAIs compared to controls.[113] In another study performed by Eirik Hagtvet et al,

liposomal doxorubicin (Caelyx®) was labelled with a lipophilic carbocyanine dye (DiD) and administered intravenously to tumour bearing mice. Then, small animal fluorescence optical imaging was used to the bio-distribution of the labelled liposomes. Results showed gradual accumulation of the liposomes achieving a plateau after 48h. However, the lack of specificity of marking NPs with dyes was illustrated by the loss of dye from the liposomes during circulation with high levels of scattering and fluorescent signal absorption. Moreover, quantitative link between the biodistribution profile of the liposomes and the doxorubicin could not be achieved.[100] In addition, fluorescence labelling can alter the biodistribution profile. For example, Patricia Álamo et al covalently attached ATTO488 (ATTO) and Sulfo-Cy5 (S-Cy5) to CXCR4-targeted self-assembling protein nanoparticles (known as T22-GFP-H6). Then, the biodistribution profile of the labelled NPs was compared to non-labelled ones in different CXCR4+ tumour mouse models. An alteration in the biodistribution profile was found where, labelled T22-GFP-H6-ATTO and T22-GFP-H6-S-Cy5 nanoparticles were accumulated in non-target organs as liver or kidney while non-labelled T22-GFP-H6 nanoparticles accumulated in CXCR4+ tumour cells.[114]

6.3.2 Fluorescence molecular tomography (FMT)

Although 2D-fluorescence reflectance imaging (FRI) is an excellent method for tracking fluorescent molecule loaded into NPs after *in vivo* administration, it cannot quantify the particles accumulated in deep tissues.[115] FMT, on the other hand, benefits from animal trans-illumination instead of surface illumination used in FRI. Lasers are used to excite NIR fluorescent molecule administered to animals at almost 120 spatial locations, then planar detectors as CCD chip cameras detect excitation and emission images (figure S3).[110] FMT offers 3D volumetric imaging by reconstructing the accumulation and concentration of fluorescent molecules thus enabling quantitative analysis of NIRF-labelled NPs in deep tissues.[98] This is achieved by obtaining enough numbers of independent experimental data from the number of light sources (set at various positions and focused on the surface) and the number of used detectors (source-detector pairs). Data obtained is sufficient to mathematically model and reconstruct quantitative distribution of all fluorescence sources in the subject. [98,111,116] However, FMT has a key drawback of being unable to allocate the built fluorescent signal to the deep organ, which made difficult its use for NPs quantification. This can be attributed to a lack of anatomical information and auto fluorescence in the background tissues that make the signal unclear.[117–119] Currently from our knowledge there is no paper reporting *in vivo* use of FMT for the tracking of organic nanoparticles.

6.3.3 Hybrid methods

A hybrid system of both FMT and computed tomography (CT) overcome drawbacks of 2D FRI and 3D FMT imaging. Indeed, this hybrid system combines anatomical information at high resolution *via* CT with highly sensitive functional and molecular information using FMT. Thus, it provides better accuracy and imaging potential in deeper tissues.[112] NIR-labelled polymeric carrier (pHPMA-Dy750) was intravenously injected to CT26 tumour-bearing mice to detect its EPR-mediated tumour accumulation. Hybrid CT-FMT showed that mice having high levels of tumour vascularisation (determined from contrast-enhanced functional ultrasound) displayed a higher level of pHPMA-Dy750 tumour accumulation (9.7% of injected dose). On the other hand, a lower level of tumour vascularisation was associated with a significant lower level of tumour accumulation (6.9% of injected dose in reconstructed CT-FMT images).[120,121]

FRI, FMT or hybrid methods like CT-FMT are interesting and easy methods for PK studies. Relevant fluorescent dyes just need to be incorporated into NPs to label and follow them into a body after injection. All these methods

allow to perform whole body studies. However due to the lack of deep resolution, it can be hard to precisely quantify a concentration of NPs following the time *in vivo*. Moreover, as for the previous methods, these fluorescent studies do not inform about the integrity of the NPs after injection into a body. Nevertheless, this issue could be overcome thanks to Förster resonance energy transfer studies (FRET) (see below part 6.5).

6.4 Microscopy imaging

Fluorescent probes can also be used for *ex vivo* experiments to characterise cellular uptake and intracellular distribution using either using fluorescence or confocal microscopy.

6.4.1 Fluorescence Microscopy

In fluorescence microscopy, visible light passes through an excitation filter, which only permits wavelength absorbed by the fluorescent molecule to cross. Then, a dichroic mirror reflects this excitation wavelength to hit the sample. After fluorescent molecule excitation, it emits a light with a larger wavelength, which is then passed through the dichroic mirror to be transmitted to the detector.[122] Fluorescence microscopy has been used to detect the cellular uptake and intracellular distribution of fluorescently labelled NPs. Texas-red labelled insulin nanocapsule for example was intragastrically administered to male Wistar rats. After 90 min, the animals were sacrificed and the ileum was isolated; cells were labelled to identify M-cells and Peyer's patches and was set for fluorescence microscopy. Bright concentrated spots of fluorescence were detected in intestinal epithelium free from M-cells. Peyer's patches showed diffused fluorescence in subjacent tissues, which indicates fluorescent insulin release from nanocapsule to the surrounding tissue. Based on fluorescence and transmission electron microscopy observations, this study showed the intestinal absorption of biodegradable nanocapsules leading to the transport of insulin across the epithelium mucosa.[107]

6.4.2 Confocal Microscopy

Laser-scanning confocal microscopy (LSCM or CLSM) offers many advantages over fluorescence microscopes. It has the ability to eliminate or decrease background noise from the focal plane, control the depth of the field, deliver specific location identity and 3D structure modelling. CLSM uses laser instead of white light source, which passes through a pinhole opening instead of an excitation filter. This pinhole aperture ensures that light reaching the detector comes only from the equivalent (confocal) point in the specimen where the excitation light was focused. Once excited, fluorescent molecules will emit light with larger wavelength and before reaching the detector, another pinhole filter is crossed to eliminate any background noise.[93,123] For example, confocal microscopy was used to study the biodistribution and elimination of dendrimer-Cy5 conjugates in intracranial rodent gliosarcoma model. Animals were injected in tail veins and euthanised at fixed time points (15 min, 1 h, 4 h, 8 h, 24 h and 48 h). Organs were harvested and placed in 4% formalin before making 30 µm-thick slices. It was found that dendrimer-Cy5 conjugates were accumulated selectively in the intracranial brain tumour 15 min after systemic administration. Homogeneous distribution in the entire tumour and peritumoral area was observed for at least 48h with gradual accumulation in tumour-associated macrophages (TAM). For authors, these results indicate that dendrimers may allow selective drug delivery to brain tumours with fast elimination from non-targeted organs.[103] Chitosan (CS) nanoparticles were also tested for ocular delivery by examining their interaction with the ocular mucosa. Chitosan was covalently attached to fluorescein *via* an amide bond. Then fluorescein labelled NPs (CS-fl) was administered to the cul-de-sac of conscious rabbits. Two hours after instillation, rabbits were sacrificed and the conjunctiva was excised and examined by a confocal microscope. Qualitative results were obtained indicating NPs penetration into the

conjunctival epithelia, which make CS-NPs a promising approach for ocular delivery.[124]

6.4.3 Two-photon fluorescence microscopy (2-PFM)

Two-photon excitation is a fluorescence technique in which the excitation of a fluorophore (a molecule that fluoresces) is excited by two photons in a simultaneous absorption process. The usual one-photon fluorescence process (e.g. confocal microscopy) depends on the excitation of a fluorophore from a ground to an excited state using a single photon. The photons applied in this process are usually in the ultraviolet or blue/green spectral range. However, in 2-PFM, the excitation can be produced using photons of less energy (typically in the infrared spectral range) under appropriate intense laser illumination. For this non-linear process to happen, the sum of energies of the two photons should be greater than the energy gap between the ground and the excited states of the fluorophore. Moreover, 2-PFM offers many advantages compared to single photon scanned imaging: (i) absorption can be confined to a very small volume at the focus of the lens (ii) best way for collecting 3D information by the use of the lowest time-integrated dose of radiation on the volume of interest (iii) Applying a longer wavelength as IR allows for less scattering and absence of autofluorescence thus no pinhole is required leading to a high fluorescence collection efficiency (iiii) excitation beam has high depth penetration (iiiii) photobleaching and photo damage is dramatically reduced, leading to a better viability of the biological specimens which can be beneficial in long-term imaging. For these reasons, two photons imaging can be used *in vivo* while confocal microscopy is only employed *ex vivo*.[125–128] In a study performed by Gao et al, organic NPs were encapsulated with two dyes using (1,2-distearoyl–sn – glycero-3-phosphoethanolamine- N – [maleimide (polyethylene glycol)-2000]) (DSPE-PEG-Mal) as the encapsulation matrix used for Diketo-Pyrrolo-pyrrole (DPP-2) encapsulation. DPP-based red-emitting AIE material displays a large stokes shift, acceptable biocompatibility and elevated brightness which allow them to be an encouraging fluorescent material for *in vivo* imaging. Retro-orbital injection of DPP-2 nanoparticles was performed and followed by the blood vasculature imaging in the mouse ear using a two-photon microscope with a depth reaching 80 µm. Bright red fluorescence was observed in the total blood vasculature network in the designated part of the dermis of the mice ear. Additionally, small capillaries and deeply placed arteries were evidently defined using DPP-2 nanoparticles.[129] In 2020, Perdoor *et al.* were able to observe the *in vivo* transcranial flow of individual NPs through the bloodstream 30 seconds after injection in a mouse.[130] In another study, Alifu *et al.* showed that two-photon fluorescence imaging can be used for *in vivo* tracking of organic NPs up to 1200 µm in the brain blood vessels of a mouse.[131] These two studies look very promising for *in vivo* use, as 2-PFM can be employed either for imaging ear blood vessel or for brain blood vessels. The only drawback for brain imaging is that this technique requires surgery which is invasive compared to whole-body imaging.

6.5 Förster (fluorescence) resonance energy transfer (FRET)

6.5.1 Basic principle of FRET

FRET is a specific fluorescence technique that depends on the transfer of energy between two fluorescent molecules. One of these fluorescent molecules is the donor (excited molecules) and the other is the acceptor. The distance between the donor and the acceptor is important for energy transfer to take place and it should not exceed 1–10 nm range. FRET signal is produced when the emission spectrum of the donor overlaps with the excitation spectrum of the acceptor followed by subsequent detected emission as shown in figure 5.[108,132–135]

Then, FRET efficiency can be defined as the part of donor molecules that transfer excitation energy to acceptor molecules. FRET efficiency is

used to assess the proximity between donor and acceptor molecules and it increases when both donor and acceptor molecules become in close proximity (typically a range of 1–10 nm). To calculate FRET efficiency (also called proximity ratio), the following equation is used:

$$PR = A / (A+D)$$

Where PR is proximity ratio, A and D are highest fluorescence intensity of acceptor and donor respectively.[136]

6.5.2 Donor-acceptor selection

Different FRET pairs can be entrapped, or covalently conjugated to NPs. However, adequate fluorescent molecule selection should consider the setting in which the study is held whether it is *in vivo* or *in vitro*. NPs face more

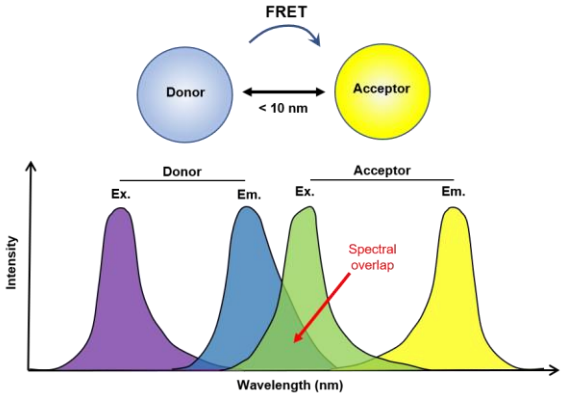

Figure 5 Different requirements for FRET detection; donor emission spectra overlapped with the acceptor excitation spectra and the two fluorescent molecules appear in a close proximity (1-10 nm). Adapted from [135]

complicated environment *in vivo* leading to weak photon penetration and important tissue auto fluorescence. Therefore, fluorescent molecules with high sensitivity, suitable depth for tissue penetration and low background fluorescence are preferable for FRET *in vivo* studies, such as cyanine dyes (i.e. DiD, DIR, DiO, Cy5.5, Cy7.5). Tracers like DiD/DiR, Cy5.5/Cy7, Cy5.5/Cy7.5, DIO/Rhodamine B and Coumarin 6/DiI are often used in FRET experiments.[133,135] Cyanine dyes are characterised by their high fluorescence stability, improved separation from auto fluorescence and less harmful effects to the cell if compared to other dyes as Coumarin 6, and Rhodamine B. Yet, unwanted aggregation, photobleaching and protein binding can influence its fluorescence spectra and quantum yield. In recent days, alternatives to conventional FRET pairs have been introduced. Among them are fluorescent molecules with aggregation-induced emission (AIE) characteristics as tetraphenylethene (TPE).[137]

6.5.3 *In vivo* fate of NPs detected by FRET

FRET was employed to study unimer-unimer and unimer-drug association in poly (ethylene glycol)-poly (D, L-lactic acid) (PEG-PDLLA) and poly (ethylene glycol)-poly (γ-propargyl-L-glutamate) (PEG-PPLG) micelles *in vivo.* First, unimers were labelled with two azide functions near-infra red dyes Cy5.5 and Cy7 where PEG-PPLG-Cy5.5 and PEG-PPLG-Cy7 were obtained. After polymeric micelle preparation, the labelled micelles were administered to BALB/C female mice *via* tail vein. *In vivo* fluorescence imaging was performed and showed micellar dissociation in real time. After blood and organ collection, the biodistribution profile showed that large portion of intact micelle remained in the circulation (44% recovered fluorescence) after 24 h, while reduced amounts were in clearance organs (33% recovered fluorescence in the liver, 11% in spleen, and 4% in kidneys). FRET efficiency of the micelles in the blood circulation was between 50 and 85% up to 72 h (initial efficiency prior to the administration was 94%).[138]

On the other hand, Cy7 labelled unimers were encapsulated by Cy5.5 dye as a drug model to study unimer-drug association. Data obtained from *in vivo* imaging illustrated the stability of FRET drug-loaded polymeric micelles. After blood and organs collection, more FRET signal was quantified in the mononuclear phagocyte system (53% recovered fluorescence in the liver, 12% in the kidney) after 8 h. FRET efficiency from isolated blood indicates that only 37% remain associated with the drug carrier (efficiency prior to administration was

85%). Authors concluded that the presence of Cy5 (drug model) affects the micelle-unimer equilibrium upon contact with the blood, unlike empty micelles which shows better stability.[138]

FRET was also applied to study *in vivo* nanoemulsion integrity. Two near-infra red dyes Cy5.5 and Cy7.5 were encapsulated into nanoemulsions. Whole animal imaging was performed after nanoemulsion retro-orbital injection to healthy and tumour bearing mice. It was found that nanoemulsion integrity was maintained in the blood of healthy mice at 93% 6h post administration while in the liver, the integrity fell to 66%. In case of a tumour, nanoemulsions entered in almost intact form (77% integrity at 2h) and at 6h, their integrity dropped to 40%. Thus, authors conclude that nanoemulsions stay intact in the blood and start to lose their integrity gradually upon entry to the tumour.[139]

Despite its poor spatial resolution, FRET imaging is a modality which is totally usable for the *in vivo* tracking of NPs. To have FRET phenomenon, the NPs need to be formulated with a pair of donor-acceptor dyes encapsulated inside. The two dyes must be sufficiently close each other, thus allowing the excitation of the acceptor dye by the donor emission wavelength. This technique is very valuable to follow the integrity of NPs. Beyond some MRI studies [140,141], it is from our knowledge the only technique which can evaluate the full integrity of the NPs with a such high degree of specificity both *in vitro* and *in vivo*. The FRET technique may also permit a quantification of the NPs in blood and organs after administration and opens a new field for studying the biodistribution of NPs.

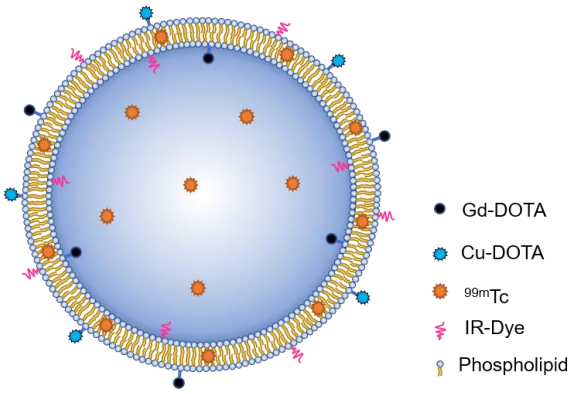

Figure 6 Schematic diagram of multifunctional liposomes. Adapted from [142]

7 - Multimodal Analysis

Combining multiple imaging techniques can offer synergistic advantages compared to employing a single modality. Thus, multimodal NPs incorporating several imaging probes are being developed to improve visualisation and data reliability.[54] An example that illustrates the advantages of multimodal analysis is the preparation of a multiprobe liposome. Since liposomes encompasses versatile modifiability, functional moieties can be incorporated into the core, linked to the surface or inserted in the phospholipid bilayer.[142] Multifunctional liposomes containing near-infrared (NIR) fluorescent tracer IRDye-DSPE, radiolabeled with ^{99m}Tc or ^{64}Cu for SPECT or PET and DSPC/cholesterol/Gd-DOTA-DSPE/DOTA-DSPE for MRI studies were prepared (figure 6).

In vivo behaviour was tracked exploiting the intrinsic advantage of each technique. MR imaging offered 3D high-resolution images of intratumoral distribution and local retention of the liposomes, while NIR fluorescence imaging showed high sensitivity and allowed local retention and systemic distribution at superficial areas to be followed. Additionally, quantitative distribution of radionuclides was obtained using nuclear imaging techniques and its lower resolution was compensated with MRI

images allowing structure and function association.[142]

These versatile designs of NPs seem to be very promising tools for PK studies using imaging methods which allow to co-locate the NPs. However, the development of such objects can be hard since it necessitates a lot of characterisations to make sure the NPs and the labelled molecules are stable over time. Overall, the development and validation of multimodal nanoparticles are currently of great research interest. In this way, one could dream that current PK studies issues (lack of sensitivity and/or spatial resolution) could be overcome in a close future, thanks to well-characterised NPs and well-established imaging protocols.

8 - Future perspective

In this review, different methods have been described for the tracking and quantification of organic NPs after *in vivo* injection (Table 2). Some of these methods are widely used in studies of the NPs' PK profile, particularly those where only blood quantification is needed.[6] As an example, indirect methods using encapsulated drug dosages are commonly used for studying the PK profile modifications induced by nanoformulations. Because these methods only give relative information to the total drug concentration and are based on extrapolations, they are not fully suited for the evaluation of the PK profile of full integrity NPs.
Other studies try to determine NPs tissue biodistribution to understand how the body deals with NPs and how the NP formulations can affect the drug effectiveness.[6] NPs biodistribution studies can be performed either upon whole animals and/or collected organs or tissue homogenates after NPs administration.
Methods using whole-body imaging are particularly interesting for the *in vivo* organic NPs detection during PK studies. Even if an increasing number of studies are currently using these techniques to follow up the biodistribution of NPs, it should be noted that each of them does not deliver the same level of information and may cause misinterpretations.
Indeed, nuclear imaging such as PET or SPECT are some of the imaging modalities which have the best sensitivity threshold (up to 10^{-12} M). However, these methods require the use of ionising radiation and suffer from a lack of spatial resolution. Hopefully, this spatial resolution issue can be overcome when PET or SPECT techniques are combined with other modalities like CT or MRI. CT scans are often combined with PET or SPECT because of the high spatial resolution abilities and the well suitability for bones and tumour imaging. Despite these advantages, PET/CT and SPECT/CT suffer from drawbacks like the double need of using ionising rays which could be an issue for longitudinal PK studies. On the other hand, MRI does not use any ionising radiation and its spatial resolution is even better compared with CT scans (25-100 µm and 50-200 µm respectively). Moreover, MRI has versatile abilities for soft tissues contrast and three-dimensional images can be obtained with anatomical information. Thus, all these advantages make MRI helpful either for morphological or functional imaging studies. Finally, the lack of sensitivity of MRI can be overpassed with dual modality techniques like PET/MRI which tend to be more and more popular with time. Unfortunately, the use of such methods is still minor over the world due to the relatively novelty of the technology and the high cost of the machines.
Another imaging modality mainly used in the literature is based on fluorescence principle. It could be explained by the fact that fluorescence techniques are often more simple and cheaper to deal with compared to the other ones. Even if it can suffer from a lack of tissue penetration and a lower spatial resolution compared to MRI, fluorescence imaging is a quite interesting technique thanks to its good sensitivity. Some relatively new techniques using microscopy like the two-photon excitation imaging look very interesting in regards with the excellent spatial resolution (up to 200 nm laterally and 1000 nm

axially) and their potential for *in vivo* tracking of organic NPs. Unfortunately, despite the relatively great tissue penetration depth for microscopy (up to 1 mm), this technique can be invasive as it can require surgery to obtain well-defined images (i.e. for brain imaging). Moreover, this technique obviously does not allow to perform whole body NP tracking in comparison with the other techniques.

All in all, none of these imaging techniques is perfect and it appears that, depending on which PK information researchers are looking for, each of these techniques will gain to be used in a synergistic way with the others in the future.

More and more studies tend now to combine the advantages of all these techniques by developing novel type of NPs dedicated to *in vivo* tracking with a multimodal imaging. This could represent a next big step for PK studies of NPs even though it becomes crucial but very challenging to have well-characterised NPs directly linked with well-validated imaging protocols. Indeed, the simple fact of thinking about multimodality means that every uncertainty factor relative to each individual technique will have to be considered and mastered. Multimodality involves so much complexity in an experiment that the number of uncertainties can increase a lot in comparison with just one imaging modality. As consequences, the multimodal imaging requires robust protocols for the synthesis/characterisation of multimodal-NPs or for the acquisition and post-treatment of

		Nuclear Imaging				Fluorescence				
									Microscopy	
	Liquid Chromatography	Positon Emission Tomography (PET)	Single Photon Emission Computed Tomography (SPECT)	Computerized Tomography (CT)	Magnetic Resonance Imaging (MRI)	Fluorescence Reflectance Imaging (FRI)	Fluo Molecular Tomography (FMT)	Förster Resonance Energy Transfert (FRET)	Confocal	Two-photons excitation imaging
Spectral range (radiation detected)	Ultraviolet (UV), visible	High energy : γ-rays	Low energy : γ-rays	X-rays	Radiowaves	Mainly red to near infrared (NIR)				Mainly visible
Tissue penetration	×	Whole body	Whole body	Whole body	Whole body	Few millimeters to centimeters			Micrometers	Up to 1 millimeter
Spatial resolution	×	1 – 2 mm	1 – 2 mm	50 – 200 µm	25 – 100 µm	1 – 2 mm			200 nm laterally 500 nm axially	200 nm laterally 1000 nm axially
Temporal resolution	Minutes to hours	10s to minutes	Minutes	Real-time to minutes	Minutes to hours	Seconds to minutes				
Sensitivity (towards drug and/or CA)	10^{-6} – 10^{-12} Mol/L	10^{-11} - 10^{-12} Mol/L	10^{-10} - 10^{-11} Mol/L	10^{-2} – 10^{-3} Mol/L	10^{-3} – 10^{-5} Mol/L	10^{-5} – 10^{-6} Mol/L				
Contrast agent quantity needed	Micrograms to nanograms	Nanograms	Nanograms	Milligrams to micrograms	Micrograms to nanograms	Micrograms to nanograms				
Specificity (tracking only organic NPs with full integrity)	+	+	+	+	+	+	+	+++	++	++
In vivo / Ex vivo	- / +	+ / +	+ / +	+ / +	+ / +	+ / +	+ / +	+ / +	- / +	+ / +
Invasiveness	+++ (*ex vivo*)	++ (ionizing rays)	++ (ionizing rays)	++ (ionizing rays)	+	+	+	+	+++ (*ex vivo*)	+++ (i.e. brain imaging)
Destructiveness	+++	-	-	-	-	-	-	-	-	-
Cost	++	+++	++	++	+++	+	+	+	++	++
Main uncertainties factors	Tissue preparation & extraction procedure	Lack of spatial resolution	Lack of spatial resolution	Concentration of contrast agent / Hardware and physical settings	Protocols settings (acquisition + post-treatment)	Lack of spatial resolution (for FRI, FMT and FRET) / Fluorescence signal highly depends on the molecular environment of the fluorophore (light scattering in tissues) / Background tissue fluorescence (autofluorescence) / Degradation of fluorophore during imaging (photobleaching)				
Resume +	Sensitive / Quantitative	Sensitive / Quantitative	Many available probes (compared to PET)	High spatial resolution / Well suited for bones and tumors	Highest spatial resolution (for whole body *in vivo* studies) / Suited for morphological and functional imaging	Sensitive / Cheap method		FRET can certify the presence of entire NPs (high specificity) / Sensitive / Cheap method	High spatial resolution / Sensitive	High spatial resolution/ Sensitive/Efficient light detection (low scattering in tissues and bkg signal strongly suppressed) / Reduced photobleaching
Resume -	Only for *ex vivo* studies / Indirect and destructive methods / Cannot certify the presence of entire NPs (lack of specificity)	Ionizing / Lack of spatial resolution / PK depend on radionuclides half-life / Need a cyclotron (cost) / Cannot certify the presence of entire NPs (lack of specificity)	Ionizing rays / lack of spatial resolution / Cannot certify the presence of entire NPs (lack of specificity)	Ionizing rays / Not suited for soft tissues / Lack of sensitivity / Cannot certify the presence of entire NPs (lack of specificity)	Low sensitivity / Lower temporal resolution / Cost	Poor spatial resolution / Cannot certify the presence of entire NPs (lack of specificity)		Poor spatial resolution	Only suited for *ex vivo* studies / Not suitable for whole body imaging	Can be invasive (i.e. for brain vessels imaging) / Not suitable for whole body imaging

Table 2: Summary and comparison of the main advantages and drawbacks of the current techniques used for the tracking of organic NPs.

imaging data. Thus, the future reproducibility of multimodal experiments will strongly depend on the control of these factors. As reproducibility is one of the key factors in imaging studies, it is important to note that a lot of research efforts still to be accomplished in this area to improve it. More studies should then be focused on the robustness quantification of their imaging protocols.

Currently, one of the biggest issues of all PK studies with organic NPs is related to the non-reflectiveness of the tracer for the NPs biodistribution. It is actually very complicated to ensure that the imaging dye added into the particles before *in vivo* injection, is still associated after injection. Thus, the release of the encapsulated dye and the stability of the NPs remain crucial steps to knock down. In other words, one of the biggest challenges in PK studies for the next years will be to find ways to characterise the integrity of NPs after *in vivo* injection.

Overall the methods described in this review, FRET seems to be one of the most promising to address this issue since it can reflect the NP integrity and structural alterations overtime whether in PK profile studies in the blood or in NPs biodistribution studies. FRET, however, still needs validated methods to extract and quantify NPs in biological fluids and tissues. In the future, a lot of work will have to be done to overcome the current issues in PK studies in nanomedicine.

9 - Conclusion

Plenty of methods and techniques have been described in the literature to study the PK profile of organic NPs and more precisely their biodistribution *in vivo*. Nuclear imaging techniques have the best sensitivity and are very suitable for biodistribution and quantification studies of NPs, while CT and MRI have the best spatial resolution for whole-body imaging. MRI is particularly interesting for the longitudinal studies dedicated to NPs tracking, thanks to its ionising radiation-free and soft contrast tissues abilities. However, all these methods are focusing on the detection of a molecular entity encapsulated or adsorbed in or on the NP and cannot fundamentally reflect the detection and an accurate quantification of NPs in a biological environment. The use of a multimodal analysis would allow to reach this issue but a lot of research efforts have to be accomplished to solve the reproducibility and the robustness issues. Finally, only the FRET technique can precisely track organic NPs with full integrity and may probably be the future of the detection and quantification of NPs for PK studies in the field of nanomedicine.

Disclosures: This work was supported by the Ligue Contre le Cancer, Maine-et-Loire Committee (49), Angers, France (#JPB/FP – 223/12.2020). Samuel Bonnet was financially supported by Biogenouest (http://www.biogenouest.org) at the University of Angers. The authors declare to have no conflict-of-interest.

Executive Summary

Introduction

- Multiple methods have been employed in tracking organic NPs *in vivo*.
- However, these techniques vary in the level of obtained information, advantages and disadvantages which may lead to misinterpretations.

Drug concentration measurement

- It is considered as indirect methods that can be used to evaluate the biodistribution of NPs.
- It involves analytical methods with or without separation processes and necessitates tissue sample preparation for solubilisation and extraction of the drug.

- However, this technique does not reflect the PK profile of the NPs themselves.

Nuclear imaging

- Nuclear imaging are whole-body techniques that are suitable for *in vivo* tracking of organic NPs by using radioisotopes.
- These techniques suffer from a lack of spatial resolution, they often need to be combined with another technique (CT or MRI).
- Nuclear imaging techniques do not ensure that the obtained signal is due to a fully intact NP, or to the NPs that are broken as only the labelled part is detected.

Computed tomography (CT)

- Computed tomography (CT) uses X-rays to provide a 3D cross-sectional tissue image with the use of contrast agents (i.e. iodine or barium-based agents) to enhance the sensitivity.
- This whole-body technique is suitable for *in vivo* tracking of organic NPs but it cannot certify the presence of fully intact NP.

Magnetic resonance Imaging (MRI)

- MRI is a nuclear magnetic resonance technique that allows for *in vivo* whole-body imaging with high spatial resolution and multi-contrast features.
- However, MRI suffers from its lack of sensitivity and its difficulty in the quantification of the contrast agents.

Fluorescence imaging

- Fluorescence Reflectance Imaging (FRI) or Fluorescence molecular tomography (FMT) is whole-body imaging technique that only provides semi-quantitative information without quantification of NPs accumulated in deep tissues. FRI and FMT allow for following organic NPs, but it is difficult to quantify them *in vivo* due to lack of spatial resolution. Moreover, it does not provide information about NPs integrity.
- **Confocal microscopy** is only employed in *ex vivo* imaging due to the lack of tissue penetration. However, the latter is only able to follow NPs in small tissue depth (i.e. mice ears) and not sufficient to track NPs in whole body without organs extraction and performing *ex vivo* studies.
- **FRET** is a specific fluorescence technique that depends on the energy transfer between two fluorescent molecules which can only occurs when the distance between the two molecules does not exceed 1-10 nm. FRET is the only technique able to track the NPs integrity *in vivo* with a high level of specificity and allows the quantification of NPs in both organs and blood. FRET is considered very promising for studying the NPs biodistribution.

Multimodal imaging

- This technique offers a synergistic advantage of multiple techniques over an individual one. However, the development of a multimodal NPs can be difficult as it needs a lot of characterisation to ensure the NPs and the labels are stable over time.

Perspectives

- Future studies aiming to evaluate the biodistribution of NPs should focus on both the quantification of imaging protocols robustness and the characterisation of NPs' integrity after *in vivo* injection.
- FRET and multimodal imaging seem to be the most promising techniques for studying the PK profile of NPs.

References

1. Lammers T, Rizzo LY, Storm G, Kiessling F. Personalized Nanomedicine. *Clin Cancer Res*. 18(18), 4889–4894 (2012).

2. Desai N. Challenges in development of nanoparticle-based therapeutics. *AAPS Journal*. 14(2), 282–295 (2012). ******

   This paper displays the complex nanoparticle behavior and the challenges facing the development of nanoparticle-based therapeutics.

3. Bertrand N, Leroux J-C. The journey of a drug-carrier in the body: An anatomo-physiological perspective. *J. Control. Release*. 161(2), 152–163 (2012).

4. Soares S, Sousa J, Pais A, Vitorino C. Nanomedicine: Principles, Properties, and Regulatory Issues. *Front. Chem*. 6 (2018).

5. Couvreur P. Nanomedicine: From where are we coming and where are we going? *J. Control. Release* 311–312, 319–321 (2019).

6. Raza K, Kumar P, Kumar N, Malik R. Pharmacokinetics and biodistribution of the nanoparticles. *Adv. Nanomed. Delivery Ther. Nucleic Acids*, 166–186 (2017).

7. Flühmann B, Ntai I, Borchard G, Simoens S, Mühlebach S. Nanomedicines: The magic bullets reaching their target? *Eur J Pharm Sci*. 128, 73–80 (2019).

8. Moss DM, Siccardi M. Optimizing nanomedicine pharmacokinetics using physiologically based pharmacokinetics modelling. *Br. J. Pharmacol*.. 171(17), 3963–3979 (2014).

9. Romero G, Moya SE. Synthesis of organic nanoparticles. In: Frontiers of Nanoscience (Volume 4): Nanobiotechnology - Inorganic Nanoparticles vs Organic Nanoparticles. de la Fuente J, Grazu V (Eds). Elsevier, Amsterdam, Netherlands, 115-141 (2012). *****

   This paper discusses different types of organic NPs and their synthesis which is the focus in this review.

10. Bisso S, Leroux JC. Nanopharmaceuticals: A focus on their clinical translatability. *Int. J. Pharm*. 578 (2020).

11. Owen SC, Chan DPY, Shoichet MS. Polymeric micelle stability. *Nano Today*. 7(1), 53–65 (2012).

12. Negar Taghavi P.A., Rouhollah Khodadust UG. Poly(amidoamine) (PAMAM) Nanoparticles: Synthesis and Biomedical Applications Poli(amidoamin) (Pamam) Nanopartiküller: Sentezi ve Biyomedikal Uygulamaları. *J. Biol and Chem*. 41(3), 289–299 (2013).

13. Bisso S, Leroux JC. Nanopharmaceuticals: A focus on their clinical translatability. *Int. J. Pharm*. 578 (2020).

14. Amin MCIM, Butt AM, Amjad MW, Kesharwani P. Polymeric Micelles for Drug Targeting and Delivery. In: Nanotechnology-Based Approaches for Targeting and Delivery of Drugs

and Genes. Mishra, Kesharwani, Amin, Lyer (Eds). Elsevier Inc, Academic Press, London,United Kingdom, 167-202 (2017).

15. Yadav HKS, Almokdad AA, shaluf SIM, Debe MS. Polymer-Based Nanomaterials for Drug-Delivery Carriers. In: Nanocarriers for Drug Delivery. Mohapatra, Ranjan, Dasgupta, Mishra, Thomas (Eds). Elsevier Inc., Amsterdam, Netherlands, 531-556 (2019).

16. Owen SC, Chan DPY, Shoichet MS. Polymeric micelle stability. *Nano Today*. 7(1), 53–65 (2012).

17. Huynh NT, Passirani C, Saulnier P, Benoit JP. Lipid nanocapsules: A new platform for nanomedicine. *Int. J. Pharm*. 379(2), 201–209 (2009).

18. Shahi SR, Kulkarni MS, Karva GS, Giram PS, Gugulkar RR. Dendrimers. *Int. J Pharm Sci Rev Res* 33(1), 187–198 (2015).

19. Negar Taghavi P.A., Rouhollah Khodadust UG. Poly(amidoamine) (PAMAM) Nanoparticles: Synthesis and Biomedical Applications Poli(amidoamin) (Pamam) Nanopartiküller: Sentezi ve Biyomedikal Uygulamaları. *J. Biol and Chem*. 41(3), 289–299 (2013).

20. Malam Y, Loizidou M, Seifalian AM. Liposomes and nanoparticles: nanosized vehicles for drug delivery in cancer. *Tr. Pharmac. Sciences*. 30(11), 592–599 (2009).

21. Chen D, Lian S, Sun J, *et al.* Design of novel multifunctional targeting nano-carrier drug delivery system based on CD44 receptor and tumor microenvironment pH condition. *Drug Deliv*. 23(3), 808–813 (2016).

22. Wang T, Zhang D, Sun D, Gu J. Current status of in vivo bioanalysis of nano drug delivery systems. *J. of Pharm. Anal*. 10(3), 221–232 (2020).

23. Arms L, Smith DW, Flynn J, *et al.* Advantages and Limitations of Current Techniques for Analyzing the Biodistribution of Nanoparticles. *Front. in Pharmacol*. 9, 802 (2018).

24. Verma S, Singh SK. LC-ESI-MS/MS estimation of loratadine-loaded self-nanoemulsifying drug delivery systems in rat plasma: Pharmacokinetic evaluation and computer simulations by GastroPlus™. *J. Pharm. Biomed. Anal*. 124, 10–21 (2016).

25. Poole CF. Solid-Phase Extraction With Discs. In*:* Solid Phase Extraction. Poole (Eds). Elsevier Inc., Amsterdam, Netherlands, 1-7 (2015).

26. Moldoveanu S, David V. Solid-Phase Extraction. In: Modern Sample Preparation for Chromatography. Moldoveanu S, David V (Eds). Elsevier Inc., Amsterdam, Netherlands, 191-286 (2015)

27. Deshpande NM, Gangrade MG, Kekare MB, Vaidya V V. Determination of free and liposomal Amphotericin B in human plasma by liquid chromatography-mass spectroscopy with solid phase extraction and protein precipitation techniques. *J. Chromatogr. B: Anal. Technol. Biomed. Life Sci.* 878(3–4), 315–326 (2010). *****

This paper displays an example on drug concentration measurements as indirect method for tracking NPs biodistribution starting from sample preparation using solid phase extraction to quantification using HPLC-MS-MS.

28. Smits EAW, Soetekouw JA, Bakker PFA, Baijens BJH, Vromans H. Plasma, blood and liver tissue sample preparation methods for the separate quantification of liposomal-encapsulated prednisolone phosphate and non-encapsulated prednisolone. *J. Liposome Res.* 25(1), 46–57 (2015).

29. Smits EAW, Soetekouw JA, van Doormalen I, *et al.* Quantitative LC-MS determination of liposomal encapsulated prednisolone phosphate and non-encapsulated prednisolone concentrations in murine whole blood and liver tissue *J. Pharm. Biomed. Anal.* 115, 552–561 (2015).

30. Šimek M, Hermannová M, Šmejkalová D, *et al.* LC–MS/MS study of in vivo fate of hyaluronan polymeric micelles carrying doxorubicin. *Carbohydr. Polym.* 209, 181–189 (2019).

31. Siddiqui MR, AlOthman ZA, Rahman N. Analytical techniques in pharmaceutical analysis: A review. *Arab. J. Chem* 10, S1409–S1421 (2017).

32. Hameed BS, Bhatt CS, Nagaraj B, Suresh AK. Chromatography as an efficient technique for the separation of diversified nanoparticles. In: Nanomaterial in Chromatography, Elsevier Inc. 503-518 (2019)

33. Moreno-Arribas MV, Polo MC. CHROMATOGRAPHY | High-performance Liquid Chromatography. *Encyclopedia of Food Sciences and Nutrition*, 1274–1280 (2003).

34. Chen ZP, Zhu JB, Chen HX, Xiao YY. A simple HPLC method for the determination of bifendate: Application to a pharmacokinetic study of bifendate liposome. *J. Chromatogr. B: Anal. Technol. Biomed. Life Sci*. 857(2), 246–250 (2007).

35. Chaudhari VS, Borkar RM, Murty US, Banerjee S. Analytical method development and validation of reverse-phase high-performance liquid chromatography (RP-HPLC) method for simultaneous quantifications of quercetin and piperine in dual-drug loaded nanostructured lipid carriers. *J. Pharm. Biomed. Anal*. 186, 113325 (2020).

36. Lesniak WG, Mishra MK, Jyoti A, *et al.* Biodistribution of fluorescently labeled PAMAM dendrimers in neonatal rabbits: Effect of neuroinflammation. *Mol. Pharm*. 10(12), 4560–4571 (2013).

37. Sharp. T.R. Mass Spectrometry. In: Drug Metabolism Handbook: Concepts and Applications. Nassar A.F., Hollenberg P.F., Scatina J. (Eds). Wiley, 167-227 (2008)

38. Makarov A, Scigelova M. Coupling liquid chromatography to Orbitrap mass spectrometry. *J. Chromatogr. A.* 1217(25), 3938–3945 (2010).

39. Estella-Hermoso de Mendoza A, Campanero MA, Mollinedo F, Blanco-Príeto MJ. Comparative study of A HPLC-MS assay versus an

UHPLC-MS/MS for anti-tumoral alkyl lysophospholipid edelfosine determination in both biological samples and in lipid nanoparticulate systems. *J. Chromatogr. B: Anal. Technol. Biomed. and Life Sci*. 877(31), 4035–4041 (2009).

40. Pham X-H, Hahm E, Kang E, *et al.* Gold-silver bimetallic nanoparticles with a Raman labeling chemical assembled on silica nanoparticles as an internal-standard-containing nanoprobe. *J. All. Comp*. 779, 360–366 (2019).

41. Pérez-Medina C, Teunissen AJP, Kluza E, Mulder WJM, van der Meel R. Nuclear imaging approaches facilitating nanomedicine translation. *Adv. Drug Deliv. Rev*. 154–155, 123–141 (2020). ******

This paper discusses available radiolabeling methods, the effect radiolabeling might have on NPs biodistribution and also discuss the neglected possibility of misinterpretations that can occur due to NPs decomposition in vivo.

42. Cherry SB. Fundamentals of positron emission tomography and applications in preclinical drug development. *J. Clin. Pharmacol.* 41(5), 482–491 (2001).

43. Li Z, Conti PS. Radiopharmaceutical chemistry for positron emission tomography. *Adv. Drug Deliv. Rev*. 62(11), 1031–1051 (2010).

44. Cherry SB. Fundamentals of positron emission tomography and applications in preclinical drug development. *J. Clin. Pharmacol*. 41(5), 482–491 (2001).

45. Andreozzi E, Seo JW, Ferrara K, Louie A. Novel method to label solid lipid nanoparticles with 64Cu for positron emission tomography imaging. *Bioconjug. Chem*. 22(4), 808–818 (2011).

46. Qin S, Seo JW, Zhang H, Qi J, Curry FRE, Ferrara KW. An imaging-driven model for liposomal stability and circulation. *Mol. Pharm*. 7(1), 12–21 (2010).

47. Corvo ML, Boerman OC, Oyen WJG, *et al.* Intravenous administration of superoxide dismutase entrapped in long circulating liposomesII. In vivo fate in a rat model of adjuvant arthritis. *Biochim. Biophys. Acta - Biomembr*. 1419(2), 325–334 (1999).

48. Jai WS, Zhang H, Kukis DL, Meares CF, Ferrara KW. A novel method to label preformed liposomes with 64Cu for positron emission tomography (PET) imaging. *Bioconjug. Chem*. 19(12), 2577–2584 (2008).

49. Janib SM, Liu S, Park R, *et al.* Kinetic quantification of protein polymer nanoparticles using non-invasive imaging. *Integr Biol*. 5(1), 183–194 (2013).

50. Fukukawa KI, Rossin R, Hagooly A, *et al.* Synthesis and characterization of core-shell star copolymers for in vivo PET imaging applications. *Biomacromolecules*. 9(4), 1329–1339 (2008).

51. Pant K, Pufe J, Zarschler K, *et al.* Surface charge and particle size determine the metabolic fate of dendritic polyglycerols. *Nanoscale*. 9(25), 8723–8739 (2017).

52. Patil RR, Yu J, Banerjee SR, *et al.* Probing in vivo trafficking of polymer/DNA micellar nanoparticles using SPECT/CT imaging. *Mol. Ther*. 19(9), 1626–1635 (2011).

53. Marik J, Tartis MS, Zhang H, *et al.* Long-circulating liposomes radiolabeled with [18F]fluorodipalmitin ([18F]FDP). *Nucl. Med. Biol*. 34(2), 165–171 (2007).

54. Chakravarty R, Hong H, Cai W. Image-Guided Drug Delivery with Single-Photon Emission Computed Tomography: A Review of Literature. *Curr. Drug Targets*. 16(6), 592–609 (2015).

55. Merkel OM, Librizzi D, Pfestroff A, Schurrat T, Béhé M, Kissel T. In Vivo SPECT and real-time gamma camera imaging of biodistribution and pharmacokinetics of siRNA delivery using an optimized radiolabeling and purification procedure. *Bioconjug. Chem.* 20(1), 174–182 (2009).

56. Man F, Gawne PJ, T.M. de Rosales R. Nuclear imaging of liposomal drug delivery systems: A critical review of radiolabelling methods and applications in nanomedicine. *Adv. Drug Deliv. Rev*. 143, 134–160 (2019).

57. Paterson A. Radiation Issues in Childhood. *Encyclopedia of Diagnostic Imaging*. (4), 1575–1578 (2008).

58. Zhang Y, Sun Y, Xu X, *et al.* Synthesis, biodistribution, and microsingle photon emission computed tomography (SPECT) imaging study of technetium-99m labeled PEGylated dendrimer poly(amidoamine) (PAMAM)-folic acid conjugates. *J. Med. Chem*. 53(8), 3262–3272 (2010).

59. Laan AC, Santini C, Jennings L, de Jong M, Bernsen MR, Denkova AG. Radiolabeling polymeric micelles for in vivo evaluation: a novel, fast, and facile method. *EJNMMI Res*. 6(1), 1–10 (2016).

60. Kim J, Chhour P, Hsu J, *et al.* Use of Nanoparticle Contrast Agents for Cell Tracking with Computed Tomography. *Bioconjug Chem*. 28(6), 1581–1597 (2017).

61. Lusic H, Grinstaff MW. X-Ray Computed Tomography Contrast Agents. *Chem Rev*. 113(3), (2013).

62. Liguori C, Frauenfelder G, Massaroni C, *et al.* Emerging clinical applications of computed tomography. *Med Devices (Auckl)*. 8, 265–278 (2015).

63. Chatterjee K, Sarkar S, Jagajjanani Rao K, Paria S. Core/shell nanoparticles in biomedical applications. *Adv. Coll. Interf. Sci*. 209, 8–39 (2014).

64. Torchilin VP, Frank-Kamenetsky MD, Wolf GL. CT visualization of blood pool in rats by using long-circulating, iodine-containing micelles. *Acad. Radiol*. 6(1), 61–65 (1999).

65. Yordanov AT, Lodder AL, Woller EK, *et al.* Novel Iodinated Dendritic Nanoparticles for Computed Tomography (CT) Imaging. *Nano Lett.* 2(6), 595–599 (2002).

66. Ho Kong W, Jae Lee W, Yun Cui Z, *et al.* Nanoparticulate carrier containing water-insoluble iodinated oil as a multifunctional contrast agent for computed tomography imaging. *Biomaterials*. 28(36), 5555–5561 (2007).

67. Wang H, Zheng L, Peng C, *et al.* Computed tomography imaging of cancer cells using acetylated dendrimer-entrapped gold nanoparticles. *Biomaterials*. 32(11), 2979–2988 (2011).

68. Wang H, Zheng L, Guo R, *et al.* Dendrimer-entrapped gold nanoparticles as potential CT contrast agents for blood pool imaging. *Nanoscale Res Lett*. 7(1), 190 (2012).

69. Rabin O, Manuel Perez J, Grimm J, Wojtkiewicz G, Weissleder R. An X-ray computed tomography imaging agent based on long-circulating bismuth sulphide nanoparticles. *Nat Mater*. 5(2), 118–122 (2006).

70. Holmberg RJ, Aharen T, Murugesu M. Paramagnetic Nanocrystals: Remarkable Lanthanide-Doped Nanoparticles with Varied Shape, Size, and Composition. *J. Phys. Chem. Lett.* 3(24), 3721–3733 (2012).

71. Chou S-W, Shau Y-H, Wu P-C, Yang Y-S, Shieh D-B, Chen C-C. In Vitro and in Vivo Studies of FePt Nanoparticles for Dual Modal CT/MRI Molecular Imaging. *J. Am. Chem. Soc.* 132(38), 13270–13278 (2010).

72. Peter J. Bonitatibus J, Torres AS, Goddard GD, FitzGerald PF, Kulkarni AM. Synthesis, characterization, and computed tomography imaging of a tantalum oxide nanoparticle imaging agent. *Chem. Commun.* 46(47), 8956–8958 (2010).

73. Cormode DP, Naha PC, Fayad ZA. Nanoparticle Contrast Agents for Computed Tomography: A Focus on Micelles. *Contrast Media Mol Imaging*. 9(1), 37–52 (2014).

74. Li X, Anton N, Zuber G, Vandamme T. Contrast agents for preclinical targeted X-ray imaging. *Adv. Drug Deliv. Rev*. 76, 116–133 (2014).

75. Maurer AH. Combined imaging modalities: PET/CT and SPECT/CT. *Health Phys*. 95(5), 571–576 (2008).

76. Hallouard F, Anton N, Zuber G, *et al.* Radiopaque iodinated nano-emulsions for preclinical X-ray imaging. *RSC Advances*. 1(5), 792–801 (2011).

77. Elrod DB, Partha R, Danila D, Casscells SW, Conyers JL. An iodinated liposomal computed tomographic contrast agent prepared from a diiodophosphatidylcholine lipid. *Nanomedicine* 5(1), 42–45 (2009).

78. Torchilin VP. PEG-based micelles as carriers of contrast agents for different imaging modalities. *Adv Drug Deliv Rev*. 54(2), 235–252 (2002).

79. Varga Z, Szigyártó ICs, Gyurkó I, *et al.* Radiolabeling and Quantitative In Vivo SPECT/CT Imaging Study of Liposomes Using the Novel Iminothiolane-99mTc-Tricarbonyl Complex. *Contrast Media Mol Imaging*. 2017, 4693417 (2017). *****

This paper illustrates an example on employing SPECT combined with CT to

study the biodistribution of liposome as an organic NP *in vivo.*

80. Pan D, Caruthers SD, Chen J, *et al.* Nanomedicine strategies for molecular targets with MRI and optical imaging. *Future Med. Chem*. 2(3), 471–490 (2010).

81. Strijkers GJ, Mulder WJM, Tilborg GAF Van, Nicolay K. MRI Contrast Agents : Current Status and Future Perspectives. *Anticancer Agents Med Chem.* 291–305 (2007).

82. Hendrick RE, Haacke EM. Basic Physics of MR Contrast Agents and Maximization of Image Contrast. *J. Magn. Reson.* 44106, 137–148 (1993).

83. Xiao Y, Paudel R, Liu JUN, Ma C, Zhang Z, Zhou S. MRI contrast agents : Classification and application. *Int. J. Mol. Med.* 1319–1326 (2016).

84. Strijkers GJ, Mulder WJM, Tilborg GAF Van, Nicolay K. MRI Contrast Agents : Current Status and Future Perspectives. *Anticancer Agents Med Chem.* 291–305 (2007).

85. Ward KM, Aletras AH, Balaban RS. A New Class of Contrast Agents for MRI Based on Proton Chemical Exchange Dependent Saturation Transfer (CEST). *J. Magn. Reson*. 143(1), 79–87 (2000).

86. Zijl PCM Van, Yadav NN. Chemical Exchange Saturation Transfer (CEST): What is in a Name and What Isn't ? *Magn. Reson. Med.* 948, 927–948 (2011).

87. Chan KWY, Yu T, Qiao Y, *et al.* A diaCEST MRI approach for monitoring liposomal accumulation in tumors. *J. Control. Release*. 180(1), 51–59 (2014).

88. Lemaire L, Bastiat G, Franconi F, *et al.* Perfluorocarbon-loaded lipid nanocapsules as oxygen sensors for tumor tissue pO2 assessment. *Eur. J. Pharm. Biopharm*. 84(3), 479–486 (2013).

89. Cittadino E, Ferraretto M, Torres E, *et al.* MRI evaluation of the antitumor activity of paramagnetic liposomes loaded with prednisolone phosphate. *Eur. J. Pharm. Sci*. 45(4), 436–441 (2012). *****

This paper illustrates the application of MRI in NPs tracking *in vivo.*

90. Päuser S, Reszka R, Wagner S, *et al.* Superparamagnetic iron oxide particles as marker substances for searching tumor specific liposomes with magnetic resonance imaging. In: Scientific and Clinical Application of Magnetic Carriers. U. Häfeli, W. Shütt, J. Teller, M. Zborowski (Eds) 561–568 (1997).

91. Bo S, Yuan Y, Chen Y, *et al.* In vivo drug tracking with 19F MRI at therapeutic dose. *Chem. Commun.* 54(31), 3875–3878 (2018).

92. Ding X, Zhao H, Li C, Wang Q, Jiang J. All-in-one theranostic nanoplatform with controlled drug release and activated MRI tracking functions for synergistic NIR-II hyperthermia-chemotherapy of tumors. *Nano Res.* 12(12), 2971–2981 (2019).

93. Sanderson MJ, Smith I, Parker I, Bootman MD. Fluorescence microscopy. *Cold Spring Harbor Protocols*. 2014(10), 1042–1065 (2014).

94. Boreham A, Brodwolf R, Walker K, Haag R, Alexiev U. Time-resolved fluorescence spectroscopy and fluorescence lifetime imaging microscopy for characterization of Dendritic polymer nanoparticles and applications in Nanomedicine. *Molecules*. 22(1) (2017).

95. Dey P. Basic and Advanced Laboratory Techniques in Histopathology and Cytology. *Basic and Advanced Laboratory Techniques in Histopathology and Cytology*. (2018).

96. Al-Jamal KT, Al-Jamal WT, Wang JTW, *et al.* Cationic poly- L -Lysine dendrimer complexes doxorubicin and delays tumor growth in vitro and in vivo. *ACS Nano*. 7(3), 1905–1917 (2013).

97. Yang J, Zhang R, Radford DC, Kopeček J. FRET-trackable biodegradable HPMA copolymer-epirubicin conjugates for ovarian carcinoma therapy. *J. Control. Release*. 218, 36–44 (2015).

98. Etrych T, Lucas H, Janoušková O, Chytil P, Mueller T, Mäder K. Fluorescence optical imaging in anticancer drug delivery. *J. Control. Release*. 226, 168–181 (2016).

99. Fruchon S, Bellard E, Beton N, *et al.* Biodistribution and biosafety of a poly(Phosphorhydrazone) dendrimer, an anti-inflammatory drug-candidate. *Biomolecules*. 9(9), 1–22 (2019).

100. Hagtvet E, Evjen TJ, Nilssen EA, Olsen DR. Assessment of liposome biodistribution by non-invasive optical imaging: A feasibility study in tumour-bearing mice. *J. Nanosci. Nanotechnol*. 12(3), 2912–2918 (2012).

101. Rip J, Chen L, Hartman R, *et al.* Glutathione PEGylated liposomes: Pharmacokinetics and delivery of cargo across the blood-brain barrier in rats. *J. Drug Target*. 22(5), 460–467 (2014).

102. Xing J, Liu D, Zhou G, *et al.* Liposomally formulated phospholipid-conjugated novel near-infrared fluorescence probe for particle size effect on cellular uptake and biodistribution in vivo. *Colloids Surf. B Biointerfaces*. 161, 588–596 (2018).

103. Zhang F, Mastorakos P, Mishra MK, *et al.* Uniform brain tumor distribution and tumor associated macrophage targeting of systemically administered dendrimers. *Biomaterials*. 52(1), 507–516 (2015).

104. Yan C, Gu J, Hou D, *et al.* Improved tumor targetability of Tat-conjugated PAMAM dendrimers as a novel nanosized anti-tumor drug carrier. *Drug Dev. Ind. Pharm*. 41(4), 617–622 (2015).

105. Oddone N, Lecot N, Fernández M, *et al.* In vitro and in vivo uptake studies of PAMAM G4.5 dendrimers in breast cancer. *J. Nanobiotechnology*. 14(1), 1–12 (2016).

106. Markus MA, Napp J, Behnke T, *et al.* Tracking of Inhaled Near-Infrared Fluorescent Nanoparticles in Lungs of SKH-1 Mice with Allergic Airway Inflammation. *ACS Nano*. 9(12), 11642–11657 (2015).

107. Pinto-Alphandary H, Aboubakar M, Jaillard D, Couvreur P, Vauthier C. Visualization of insulin-loaded nanocapsules: In vitro and in vivo studies after oral administration to rats. *Pharm. Res*. 20(7), 1071–1084 (2003).

108. Roger E, Gimel JC, Bensley C, Klymchenko AS, Benoit JP. Lipid nanocapsules maintain full integrity after crossing a human intestinal epithelium model. *J. Control. Release*. 253, 11–18 (2017).

109. Bouchaala R, Anton N, Anton H, *et al.* Light-triggered release from dye-loaded fluorescent lipid nanocarriers in vitro and in vivo. *Colloids Surf B Biointerfaces*. 156, 414–421 (2017).

110. Etrych T, Janoušková O, Chytil P. Fluorescence imaging as a tool in preclinical evaluation of polymer-based nano-DDS systems intended for cancer treatment. *Pharmaceutics*. 11(9) (2019).

111. Dufort S, Sancey L, Wenk C, Josserand V, Coll JL. Optical small animal imaging in the drug discovery process. *Biochim. Biophys. Acta - Biomembranes*. 1798(12), 2266–2273 (2010).

112. Kunjachan S, Gremse F, Theek B, *et al.* Noninvasive optical imaging of nanomedicine biodistribution. *ACS Nano*. 7(1), 252–262 (2013).

113. Markus MA, Napp J, Behnke T, *et al.* Tracking of Inhaled Near-Infrared Fluorescent Nanoparticles in Lungs of SKH-1 Mice with Allergic Airway Inflammation. *ACS Nano*. 9(12), 11642–11657 (2015).

114. Álamo P, Pallarès V, Céspedes MV, *et al.* Fluorescent Dye Labeling Changes the Biodistribution of Tumor-Targeted Nanoparticles. *Pharmaceutics*. 12(11), 1004 (2020).

115. Ntziachristos V, Ripoll J, Wang L V., Weissleder R. Looking and listening to light: The evolution of whole-body photonic imaging. *Nature Biotech*. 23(3), 313–320 (2005).

116. Stuker F, Ripoll J, Rudin M. Fluorescence molecular tomography: Principles and potential for pharmaceutical research. *Pharmaceutics*. 3(2), 229–274 (2011).

117. Graves EE, Ripoll J, Weissleder R, Ntziachristos V. A submillimeter resolution fluorescence molecular imaging system for small animal imaging. *Medical Physics*. 30(5), 901–911 (2003).

118. Ntziachristos V, Weissleder R. Experimental three-dimensional fluorescence reconstruction of diffuse media by use of a normalized Born approximation. *Optics Letters*. 26(12), 893 (2001).

119. Ntziachristos V. Fluorescence Molecular Imaging. *Annu. Rev. Biomed. Eng*. 8(1), 1–33 (2006).

120. Theek B, Gremse F, Kunjachan S, *et al.* Characterizing EPR-mediated passive drug targeting using contrast-enhanced functional ultrasound imaging. *J. Control. Release*. 182(1), 83–89 (2014).

121. Chi C, Du Y, Ye J, *et al.* Intraoperative imaging-guided cancer surgery: From current fluorescence molecular imaging methods to future

multi-modality imaging technology. *Theranostics*. 4(11), 1072–1084 (2014).

122. Hell SW, Dyba M, Jakobs S. Concepts for nanoscale resolution in fluorescence microscopy. *Curr Opin in Neurobiol*. 14(5), 599–609 (2004).

123. Panula PAJ. Handbook of Biological Confocal Microscopy. *Journal of Chemical Neuroanatomy*. 25(3), 228–229 (2003).

124. De Campos AM, Diebold Y, Carvalho ELS, Sánchez A, Alonso MJ. Chitosan nanoparticles as new ocular drug delivery systems: In vitro stability, in vivo fate, and cellular toxicity. *Pharm. Res*. 21(5), 803–810 (2004).

125. Denk W, Strickler JH, Webb WW. Two-photon laser scanning fluorescence microscopy. *Science*. 248(4951), 73–76 (1990).

126. Mondal PP, Diaspro A. Multiphoton Fluorescence Microscopy. In: *Fundamentals of Fluorescence Microscopy: Exploring Life with Light*. Mondal PP, Diaspro A (Eds.), Springer Netherlands, Dordrecht, 149–159 (2014).

127. Diaspro A, Chirico G, Collini M. Two-photon fluorescence excitation and related techniques in biological microscopy. *Q Rev Biophys*. 38(2), 97–166 (2005).

128. Rubart M. Two-Photon Microscopy of Cells and Tissue. *Circ. Res*. 95(12), 1154–1166 (2004).

129. Gao Y, Feng G, Jiang T, *et al.* Biocompatible Nanoparticles Based on Diketo-Pyrrolo-Pyrrole (DPP) with Aggregation-Induced Red/NIR Emission for In Vivo Two-Photon Fluorescence Imaging. *Adv. Funct. Mat*. 25(19), 2857–2866 (2015).

130. Perdoor SS, Dubois F, Barbara A, *et al.* Ultrabright Silica-Coated Organic Nanocrystals for Two-Photon In Vivo Imaging. *ACS Appl. Nano Mater*. 3(12), 11933–11944 (2020).

131. Alifu N, Yan L, Zhang H, *et al.* Organic dye doped nanoparticles with NIR emission and biocompatibility for ultra-deep in vivo two-photon microscopy under 1040 nm femtosecond excitation. *Dyes and Pigments*. 143, 76–85 (2017).

132. Jares-Erijman EA, Jovin TM. FRET imaging. *Nature Biotech*. 21(11), 1387–1395 (2003).

133. Lainé AL, Gravier J, Henry M, *et al.* Conventional versus stealth lipid nanoparticles: Formulation and in vivo fate prediction through FRET monitoring. *J.Control. Release*. 188, 1–8 (2014).

134. Piston DW, Kremers GJ. Fluorescent protein FRET: the good, the bad and the ugly. *Trends Biochem. Sci*. 32(9), 407–414 (2007).

135. Chen T, He B, Tao J, *et al.* Application of Förster Resonance Energy Transfer (FRET) technique to elucidate intracellular and In Vivo biofate of nanomedicines. *Adv. Drug Deliv. Rev*. 143, 177–205 (2019).

136. Chen H, Puhl HL, Koushik SV, Vogel SS, Ikeda SR. Measurement of FRET Efficiency and Ratio of Donor to Acceptor Concentration in Living

Cells. *Biophys. J.* 91(5), L39–L41 (2006).

137. Wang C, Wang Z, Zhao X, *et al.* DOX Loaded Aggregation-induced Emission Active Polymeric Nanoparticles as a Fluorescence Resonance Energy Transfer Traceable Drug Delivery System for Self-indicating Cancer Therapy. *Acta Biomaterialia*. 85, 218–228 (2019).

138. Morton SW, Zhao X, Quadir MA, Hammond PT. FRET-enabled biological characterization of polymeric micelles. *Biomaterials*. 35(11), 3489–3496 (2014). *****

This paper displays the advantages of FRET in tracking organic NPs in vivo and how it can follow the integrity of a nanoparticle system over time.

139. Bouchaala R, Mercier L, Andreiuk B, *et al.* Integrity of lipid nanocarriers in bloodstream and tumor quantified by near-infrared ratiometric FRET imaging in living mice. *J. Control. Release*. 236, 57–67 (2016).

140. Lorenzato C, Oerlemans C, Elk M van, *et al.* MRI monitoring of nanocarrier accumulation and release using Gadolinium-SPIO co-labelled thermosensitive liposomes. *Contrast Media Mol. Imaging*. 11(3), 184–194 (2016).

141. Langereis S, Keupp J, van Velthoven JLJ, *et al.* A Temperature-Sensitive Liposomal 1H CEST and 19F Contrast Agent for MR Image-Guided Drug Delivery. *J. Am. Chem. Soc.* 131(4), 1380–1381 (2009).

142. Li S, Goins B, Zhang L, Bao A. Novel multifunctional theranostic liposome drug delivery system: Construction, characterization, and multimodality MR, near-infrared fluorescent, and nuclear imaging. *Bioconjug. Chem*. 23(6), 1322–1332 (2012). **

This paper shows the advantages of combining multiple imaging modalities on tracking of a multiprobe liposome which can have a great potential in future PK studies.